





RESEARCH ARTICLE

The influence of DACCIWA radiosonde data on the quality of ECMWF analyses and forecasts over southern West Africa

Roderick van der Linden¹  | Peter Knippertz¹  | Andreas H. Fink¹  | Bruce Ingleby²  |
Marlon Maranan¹  | Angela Benedetti² 

¹Institute of Meteorology and Climate Research, Karlsruhe Institute of Technology, Karlsruhe, Germany

²European Centre for Medium-Range Weather Forecasts, Reading, UK

Correspondence

R. van der Linden, Karlsruhe Institute of Technology, Institute of Meteorology and Climate Research, 76128 Karlsruhe, Germany.

Email: roderick.linden@kit.edu

Abstract

During the DACCIWA (Dynamics–Aerosol–Chemistry–Cloud Interactions in West Africa) field campaign ~900 radiosondes were launched from 12 stations in southern West Africa from 15 June to 31 July 2016. Subsequently, data-denial experiments were conducted using the Integrated Forecasting System of the European Centre for Medium-range Weather Forecasts (ECMWF) to assess the radiosondes' impact on the quality of analyses and forecasts. As observational reference, satellite-based estimates of rainfall and outgoing long-wave radiation (OLR) as well as the radiosonde measurements themselves are used. With regard to the analyses, the additional observations show positive impacts on winds throughout the troposphere and lower stratosphere, while large lower-tropospheric cold and dry biases are hardly reduced. Nonetheless, downstream, that is farther inland from the radiosonde stations, we find a significant increase (decrease) in low-level night-time temperatures (monsoon winds) when incorporating the DACCIWA observations, suggesting a possible linkage via weaker cold air advection from the Gulf of Guinea. The associated lower relative humidity leads to reduced cloud cover in the DACCIWA analysis. Closer to the coast and over Benin and Togo, DACCIWA observations increase low-level specific humidity and precipitable water, possibly due to changes in advection and vertical mixing. During daytime, differences between the two analyses are generally smaller at low levels. With regard to the forecasts, the impact of the additional observations is lost after a day or less. Moderate improvements occur in low-level wind and temperature but also in rainfall over the downstream Sahel, while impacts on OLR are ambiguous. The changes in precipitation appear to also affect high-level cloud cover and the tropical easterly jet. The overall rather small observation impact suggests that model and data assimilation deficits are the main limiting factors for better forecasts in West Africa. The new observations and physical understanding from DACCIWA can hopefully contribute to reducing these issues.

KEYWORDS

data-denial experiment, field campaign, radiosonde measurements, West African monsoon

This is an open access article under the terms of the Creative Commons Attribution License, which permits use, distribution and reproduction in any medium, provided the original work is properly cited.

© 2020 The Authors. *Quarterly Journal of the Royal Meteorological Society* published by John Wiley & Sons Ltd on behalf of the Royal Meteorological Society.

1 | INTRODUCTION

The climate of southern West Africa is characterized by the West African monsoon (e.g. Fink *et al.*, 2017). Accurate forecasts, particularly of precipitation, are of great socio-economic importance in this region, because rain-fed agriculture is practised by many smallholder farmers (Parker and Diop-Kane, 2017). In addition, recent studies have pointed out the tendency of West Africa towards extreme rainfall events that can lead to urban flooding (Engel *et al.*, 2017; Lafore *et al.*, 2017; Maranan *et al.*, 2019).

The performance of current operational weather forecasting systems over West Africa, however, is generally insufficient to provide guidance for agricultural planning and disaster prevention. Vogel *et al.* (2018) evaluate ensemble forecasts from nine global models participating in The International Grand Global Ensemble (TIGGE) project (Bougeault *et al.*, 2010) for northern tropical Africa and demonstrate that even after sophisticated statistical post-processing, forecast skill barely exceeds that of climatology-based probabilistic approaches. The authors hypothesize that one key reason is the parametrization of convection, which is hardly able to represent the physical mechanisms involved in the formation of organized mesoscale convective systems, which dominate rainfall production over large parts of West Africa (Mathon *et al.*, 2002; Dezfuli *et al.*, 2017; Maranan *et al.*, 2018). Also using TIGGE, Milton *et al.* (2017) show significant model drifts in temperature, moisture, pressure and precipitation with a tendency for rainfall overestimation at longer lead times, while Louvet *et al.* (2016) document good performance in forecasting regional-scale features such as the latitudinal shift of the main rain band and the onset of the West African monsoon. For higher-resolution deterministic forecasts, Kniffka *et al.* (2019a) find very little correlation between station observations of rainfall and collocated forecasts, while propagating synoptic-scale vortices and waves (Knippertz *et al.*, 2017) appear to enhance predictability for southern West Africa as a whole.

Many studies document fast-physics errors that cause significant biases within the first 24 hr of the forecast and negatively affect the representation of the diurnal cycle (Marsham *et al.*, 2013; Bechtold *et al.*, 2014; Kouadio *et al.*, 2018; Kniffka *et al.*, 2019b). Resulting biases in the northward advection of moisture into the Sahel and the Sahara and positive feedbacks can shift the entire main rain band latitudinally (Druyan *et al.*, 2010; Birch *et al.*, 2014). One particular problem is the sensitive relationship of deeper clouds with the land surface and the planetary boundary layer (PBL) (Couvreur *et al.*, 2014) including the extensive decks of low-level clouds over southern West Africa (e.g. Schrage and Fink, 2012; van der Linden *et al.*, 2015). These

typically form at night during the summer monsoon due to a combination of cold advection, radiative cooling and turbulent mixing underneath the nocturnal low-level jet (NLLJ), and then lift and dissolve in the course of the day (Schuster *et al.*, 2013; Adler *et al.*, 2017; 2019; Dione *et al.*, 2019). Given the significant net (mostly short-wave) radiative effect of these clouds (Hill *et al.*, 2018) and the weakly stable atmosphere, their impact on rainfall is considerable (Kniffka *et al.*, 2019b). This is consistent with Söhne *et al.* (2008) who find too many/too thick low clouds between 5 and 10°N, too cold surface temperatures, a too shallow PBL, reduced convective available potential energy and suppressed deep convection in addition to a too fast monsoon flow and too little vertical mixing, which limits speed reduction and drying.

One other important reason for the poor forecast performance over West Africa appears to be the sparse observational network (e.g. Parker *et al.*, 2008; Knippertz *et al.*, 2015). Satellite-based estimates are known to have considerable biases, as shown for example for rainfall (e.g. Thiemig *et al.*, 2012) and surface solar irradiance (e.g. Hannak *et al.*, 2017). Insufficient observational constraints combined with poor model first guesses lead to a substantial uncertainty in analysis products (Roberts *et al.*, 2015; Hill *et al.*, 2016), which negatively impacts on model initialization, forecast verification and model development.

This raises the question of whether the low forecast quality over West Africa is due to poor observations, model error or deficits in the data assimilation system. One objective way to determine this is data-denial experiments, in which additional observations from field campaigns or satellites are denied to the data assimilation system (e.g. Kelly *et al.*, 2007). Comparing such experiments with analyses and predictions using all available data allows estimation of the observation impact and can also help identify sources of model error. A seminal data-denial study for West Africa is Agustí-Panareda *et al.* (2010) based on the Integrated Forecasting System (IFS) of the European Centre for Medium-range Weather Forecasts (ECMWF). The study made use of the extensive radiosonde measurements from the African Monsoon Multidisciplinary Analysis (AMMA) Special Observing Period in August 2006 (Lebel *et al.*, 2010), which allowed a three-dimensional representation of essential weather features over West Africa. AMMA had a regional focus on the Sahel and substantially helped improve the understanding of the West African monsoon system (Lafore *et al.*, 2011). One important finding of Agustí-Panareda *et al.* (2010) is that the additional radiosonde data enhanced the African Easterly Jet (AEJ) in its left entrance region, which is known to play an important role for African Easterly Waves (e.g. Fink *et al.*, 2017) and the development of intense convective systems (e.g. Mohr and Thorncroft, 2006). Interestingly,

another data-denial study (Tompkins *et al.*, 2005) shows that impacts on the AEJ can be larger from thermodynamic information than from the wind measurements themselves in a four-dimensional variation (4D-Var) system, indicating dynamic adjustment processes. Somewhat disappointingly, however, Agustí-Panareda *et al.* (2010) do not find a clear positive impact on ECMWF forecasts over Africa beyond 24 hr, although Faccani *et al.* (2009) see a downstream propagation of forecast improvement over Europe during the first 2–3 days of the forecast (see also Pante and Knippertz, 2019). Satellite data assimilation experiments by Karbou *et al.* (2010) show 1–3-day forecast improvements in 200 hPa geopotential over Africa but rather mixed results for precipitation.

In June–July 2016 the Dynamics–Aerosol–Chemistry–Cloud Interactions in West Africa (DACCIWA) project (Knippertz *et al.*, 2015) organised an extensive field campaign in southern West Africa involving the countries Ivory Coast, Ghana, Togo, Benin and Nigeria (Flamant *et al.*, 2018). The campaign covered the period before and after the monsoon onset of that year (Knippertz *et al.*, 2017). While the main aim of DACCIWA was to improve the understanding of the interaction between anthropogenic and natural emissions, clouds, radiation, rainfall and the circulation over southern West Africa, the extensive radiosonde measurements during the campaign offer a unique opportunity for data-denial experiments similar to those by Tompkins *et al.* (2005) and Agustí-Panareda *et al.* (2010). This way an evaluation can be provided of whether and in what sense the ECMWF IFS has improved over the last 10 years, here with a specific focus on southern West Africa. Impacts of the additional observations on both the analyses and the forecasts will be assessed in this article. In Section 2, the data used in this study and the methods employed to evaluate the data-denial experiments are introduced. The influence of DACCIWA radiosonde data on the ECMWF analyses and forecasts is discussed in Sections 3 and 4, respectively. The article concludes with a summary and discussion of the main results in Section 5.

2 | DATA AND METHODS

Figure 1 shows the locations of the 12 stations from which radiosondes were launched during the DACCIWA campaign period from 15 June to 31 July 2016 (Maranan and Fink, 2016). They cover the countries of Ivory Coast, Ghana, Benin and Nigeria. All stations south of 10°N were considered for the data-denial experiments, while data from the station Kano in Nigeria (12°N) were always assimilated due to the large distance to the other stations and its location outside the core DACCIWA region. In

total, approximately 900 radiosonde ascents are available (mainly as alphanumeric reports; some as BUFR (Binary Universal Form for the Representation of meteorological data) but not at high resolution), but the availability strongly depends on the location (Table 1; cf. figures ES5 and ES6 in Flamant *et al.*, 2018). The highest numbers of radiosonde ascents were available from Accra (135 reports) and Abidjan (165 reports). There are also temporal variations. The 76 radiosonde profiles available from Lamto were all measured during an intensive operation period between 6 and 20 July with up to seven measurements per day.

Some of the reports were used in real-time operations at ECMWF but others were only received later via the Karlsruhe Institute of Technology, the institution that coordinated DACCIWA. In addition to full radiosonde ascents (wind, temperature and humidity generally reaching the lower stratosphere), some stations provided wind-only PILOT reports, typically up to 700 or 500 hPa. Figure 2 provides an overview of the availability of radiosonde measurements at different standard pressure levels for temperature and specific humidity. While the black lines show the number of all available values, the green lines depict the number of assimilated values. As can be seen, more than 1,600 observations (including duplicates) were available between 925 and 100 hPa. At 1000 hPa fewer reports were available due to several stations having lower station pressures. The number of reports is reduced in the stratosphere at and above 100 hPa. Upper-tropospheric humidity is difficult to measure well (Ingleby, 2017, and references therein) and above 300 hPa only humidity measurements from Vaisala radiosondes were assimilated (Figure 2b, green line). A more detailed overview of availability of radiosonde data from the DACCIWA field campaign is provided in figures ES5 and ES6 of Flamant *et al.* (2018).

The DACCIWA data-denial experiments were run using ECMWF IFS cycle 45r1, which became the operational model cycle on 5 June 2018. The model was run with 137 levels (model top at 0.01 hPa) on a TCo399 cubic octahedral grid, which corresponds to a grid spacing of approximately 29 km. The output was interpolated onto a 0.25° × 0.25° latitude–longitude grid for further study. The forecast model used here is coarser than the operational high-resolution deterministic version of cycle 45r1 with 9 km grid spacing. We used analyses and forecasts every 6 hr. The incremental analysis was on a TL255 grid (about 80 km) with a 12 hr 4D-Var window. The analyses at 0000 and 0600 UTC (and correspondingly at 1200 and 1800 UTC) are snapshots inside the same 12 hr assimilation window (e.g. Andersson and Thépaut, 2008). Forecasts are generally available for time steps of up to 240 hr (10 days), but the focus here will be on forecasts up to 48 hr. For forecast hours 0000 and 1200 UTC, lead times

FIGURE 1 Locations of stations in southern West Africa where radiosondes were launched during the DACCIWA field campaign between 15 June and 31 July 2016. For frequency and number of observations per station see Table 1, and figures ES5 and ES6 in Flamant *et al.* (2018). Radiosonde data from Kano (Nigeria) were used in both experiments. The shading indicates the orography

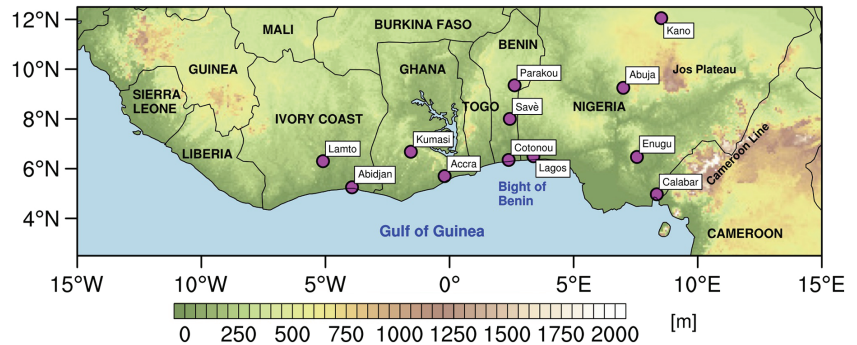


TABLE 1 Stations with radiosonde measurements during the DACCIWA field campaign between 15 June and 31 July 2016. Table 2 of Flamant *et al.* (2018) gives the radiosonde types used. Note that for some stations the rightmost column contains duplicates and additional wind information from PILOT reports, which are not counted in the second column from the right

| Country | Station name | Station identifier | Latitude [°N] | Longitude [°E] | Number of DACCIWA radiosonde profiles | Number of radiosonde profiles (temperature/wind) assimilated in DACCIWA experiment |
|---------------------|-------------------|--------------------|---------------|----------------|---------------------------------------|--|
| Ivory Coast | Lamto | IVLAM | 6.3 | -5.1 | 76 | 78/78 |
| | Abidjan | 65578 | 5.25 | -3.93 | 164 | 165/176 |
| Ghana | Kumasi | 65442 | 6.68 | -1.56 | 105 | 122/122 |
| | Accra | GHACC | 5.7 | -0.2 | 135 | 135/135 |
| Benin | Save | LA-SAVE | 8.00 | 2.43 | 98 | 98/98 |
| | Cotonou | 65344 | 6.35 | 2.38 | 105 | 95/164 |
| | Parakou | 65330 | 9.35 | 2.62 | 95 | 94/94 |
| Nigeria | Lagos | 65202 | 6.5 | 3.38 | 36 | 36/36 |
| | Abuja | 65125 | 9.25 | 7.00 | 46 | 47/47 |
| | Enugu | 65257 | 6.47 | 7.55 | 2 | 2/2 |
| | Calabar | 65264 | 4.97 | 8.35 | 12 | 10/10 |
| | Kano ^a | 65046 | 12.05 | 8.53 | 17 | 18/18 |
| Sum of measurements | | | | | 891 | 900/954 |

^aUsed in both experiments.

of 0, 6, 12, 24, 36 and 48 hr were used, while for 0600 and 1800 UTC only the lead times 0, 6, 12 and 18 hr are available.

The IFS was run with two different set-ups for the entire radiosonde period from 15 June to 31 July 2016, comprising a total of 47 days. In the first set-up, all available radiosonde observations that passed quality control were assimilated. The data were bias-corrected using the operational version of the bias-correction scheme that was originally developed by Agustí-Panareda *et al.* (2009) in the framework of AMMA. In the second set-up, all radiosonde data available in the study region (i.e. not those from Kano) were excluded from assimilation. In the following, the two experiments will be referred to as DACCIWA and noDACCIWA analyses/forecasts. All other reports that are

routinely assimilated in the IFS (i.e. data from surface, satellite and aircraft measurements) were used in both experiments. Given the sparse standard network and frequent problems with the transmission of data into international networks, the noDACCIWA run is more representative of the situation outside of field campaign activities in West Africa. As one recent example, from the whole WMO block 65 only approximately three radiosonde stations per month reported in January–July 2019 (with a recovery to about six stations afterwards). All variables used in the operational set-up of 45r1 are available for the two experiments from the ECMWF Meteorological Archival and Retrieval System (MARS) under the acronyms gwwb and gx6u for the DACCIWA and noDACCIWA analyses/forecasts, respectively.

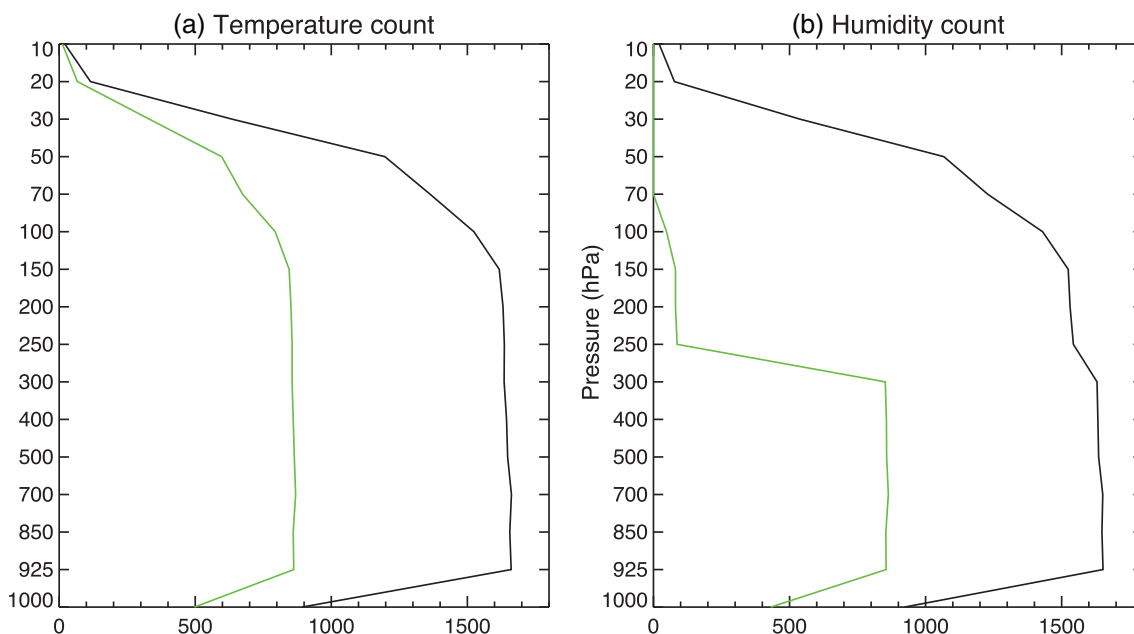


FIGURE 2 Numbers of standard level (a) temperature and (b) humidity reports in the DACCIWA experiment. Black indicates all values and green the assimilated values. Wind counts (not shown) are similar to those for temperature (or slightly higher if PILOT profiles are included). There can be (near-)duplicate reports for several reasons, most of which are excluded from the assimilation. Humidity is not assimilated in the stratosphere and is only used from Vaisala radiosondes in the upper troposphere

The DACCIWA analyses are evaluated by calculating the mean biases with respect to the noDACCIWA analyses. The DACCIWA and noDACCIWA forecasts of daily top of atmosphere (TOA) outgoing long-wave radiation (OLR) and precipitation were validated with independent observational data. For OLR and precipitation, the reference datasets were EUMETSAT Climate Monitoring Satellite Application Facility (CM SAF) TOA Emitted Thermal radiative flux (TET) version 303 (EUMETSAT, 2019) and Climate Hazards Group InfraRed Precipitation with Station (CHIRPS) 2.0 (Funk *et al.*, 2015; for a comparison with other precipitation datasets see, for example, Satgé *et al.* (2020)), respectively. CM SAF TET is available at a sinusoidal (equal-area) projection with a grid spacing of 45 by 45 km at the Equator. For CHIRPS 2.0, the version with a $0.25^\circ \times 0.25^\circ$ latitude–longitude grid was used. Both datasets were remapped to the ECMWF grid from their native horizontal resolution using conservative remapping. For the evaluation against the satellite-based datasets, ECMWF radiation and precipitation forecasts were used. Since radiation variables are provided as accumulated fluxes in MARS, daily mean TOA OLR was calculated by taking the difference between the $t + 24$ hr and $t + 0$ hr forecasts started at 0000 UTC and dividing by 86,400 s. Note that the TOA OLR from ECMWF was multiplied by -1 to get the sign matching with that of CM SAF TET. Daily rainfall was calculated by taking the difference between the $t + 36$ hr and $t + 12$ hr forecasts started at 1200 UTC. This allows accounting for model spin-up,

consistent with the approach used in Agustí-Panareda *et al.* (2010). Moreover, low-level wind speed and temperature forecasts for both experiments were validated against the DACCIWA analyses using the root-mean-square error (RMSE). Statistical significance of biases was tested with a distribution-independent bootstrapping approach with 10,000 samples. Biases that are statistically significant on the 5% level are highlighted.

3 | INFLUENCE ON ECMWF ANALYSES

In this section, the impact of the additional DACCIWA radiosonde observations on the ECMWF analyses will be discussed. As a first step, differences between the radiosonde observations (excluding Kano) and, respectively, the model background (O–B) and final analysis (O–A), averaged over all DACCIWA radiosonde stations, will be investigated and compared between the DACCIWA and noDACCIWA experiments. This serves to quantify the overall impact of the campaign on the reduction of biases and the standard deviation of the differences (Section 3.1). Subsequently, a more detailed examination of the horizontal distribution of differences between the two analyses will be presented in Section 3.2. A wide range of parameters and vertical levels was inspected but here we will concentrate on the variables showing the most coherent and statistically significant differences. These are

column moisture, low-level temperature, wind, humidity and cloud cover, as well as high-level wind and cloud cover. Section 3.2 serves to illustrate the sensitivity of the data assimilation system but does not allow a direct assessment of which analysis is actually better due to the lack of any verifying observations.

3.1 | Influence on vertical statistics of O–B and O–A at the radiosonde locations

Figure 3 shows vertical distributions of the influence of DACCIWA upper-air information on O–B and O–A statistics, respectively, both for the DACCIWA and noDACCIWA experiments. Model background in this context refers to the short-range (12 hr) integration of the IFS in the 4D-Var system.

For temperature, the background has a considerable cold bias below 500 hPa and then again above 200 hPa reaching more than 0.5 K near the surface and in the lower stratosphere, irrespective of the assimilation of DACCIWA radiosondes, which influence the background through cycling (black and pink dashed lines in Figure 3a). A cold low-level temperature bias in IFS is found throughout the Tropics (cf. figure 3.1 of Ingleby, 2017), and is thought to be linked to biases in humidity and low-cloud cover. However, over the study region the cold bias may partly also be a result of changes in temperature advection, as southern West Africa is characterised by a poleward temperature gradient and a southerly monsoon flow at low levels. Assimilating observations other than the DACCIWA radiosondes even increases the bias at both low and stratospheric levels (orange dashed line in Figure 3a). Additionally, assimilating the DACCIWA radiosondes slightly improves the bias at most tropospheric levels, with a distinct vertical shift in bias in the stratosphere (blue dashed line in Figure 3a). Looking at the standard deviations (solid lines in Figure 3a) reveals fairly constant values of almost 1 K throughout the troposphere and a marked increase in the stratosphere. Here, the positive impact of the DACCIWA radiosondes is more evident at all levels (blue solid line), while the other three curves are fairly similar. This demonstrates that while the magnitude of day-to-day errors can be moderately reduced, the bias largely remains. Overall, these results suggest substantial issues with both the IFS model and assimilation system that will be discussed further below.

The corresponding analysis for specific humidity (Figure 3b) resembles the results for temperature in many ways. Mean differences are large and positive (i.e. the IFS has a dry bias) below 500 hPa, reaching more than 0.5 g·kg⁻¹ near the surface. Data assimilation does not reduce the bias, but even increases it at some

levels, particularly if DACCIWA radiosondes are excluded (orange dashed line in Figure 3b). In contrast, the standard deviation can effectively be reduced through the radiosondes, particularly at the top of the monsoon layer, between 850 and 700 hPa, where errors are particularly large. Here a positive impact of cycling is also evident (cf. black vs. pink and orange solid lines in Figure 3b). Interestingly, the cold and dry biases combined lead to almost bias-free estimates of relative humidity up to about 400 hPa (dashed lines in Figure 3c). The negative differences above this need to be looked at with caution due to the increasingly low temperatures that also cause problems for the radiosonde humidity measurements (Ingleby, 2017, and references therein). Overall, the assimilation of DACCIWA radiosondes has little effect on relative-humidity biases. One possible explanation could be a strong linkage of lower-tropospheric biases to surface biases, which is supported by O–A and O–B biases being very similar at 1000 hPa. Nevertheless, the standard deviation shows a consistent improvement through the assimilation of DACCIWA radiosondes for the entire troposphere (blue solid line in Figure 3c).

In the tropical lower troposphere, the satellite data with the largest impact are those from microwave sounders (figure 4 in Bormann *et al.*, 2019). Although their effect is only 1–2% in terms of fit to radiosonde (standard deviation of O–B) for wind and temperature, the improvement for specific humidity is up to 6% (this is at 850 hPa). However, this improvement is at the expense of larger biases (unpublished results from Bormann *et al.*, 2019). Infrared satellite sounding data has a broadly similar impact but smaller magnitude. The use of satellite sounding data can include biases from various sources, such as the modelling of surface emissivity, that are not fully removed by bias corrections. Another issue is the low effective vertical resolution of the information from the satellite soundings, much lower than from radiosondes. If the background boundary-layer depth is wrong, then the analysis can be unrealistic as discussed by Ingleby *et al.* (2013). If the background has a different sign of humidity error within and above the boundary layer, then the lack of vertical resolution would also be a problem.

Finally, Figure 3d,e show corresponding results for the zonal and meridional wind components, respectively. Biases have a more complicated vertical structure here in both components. noDACCIWA O–B biases (pink dashed lines) are usually largest in magnitude as expected. The indirect effect of the DACCIWA radiosondes on the background through cycling (black dashed lines) leads to bias reduction at most levels, particularly in the stratosphere. Assimilating non-radiosonde information (orange dashed lines) also largely has a positive impact, which is clearest in the upper troposphere, likely due to cloud-motion vectors derived from high clouds, while stratospheric winds

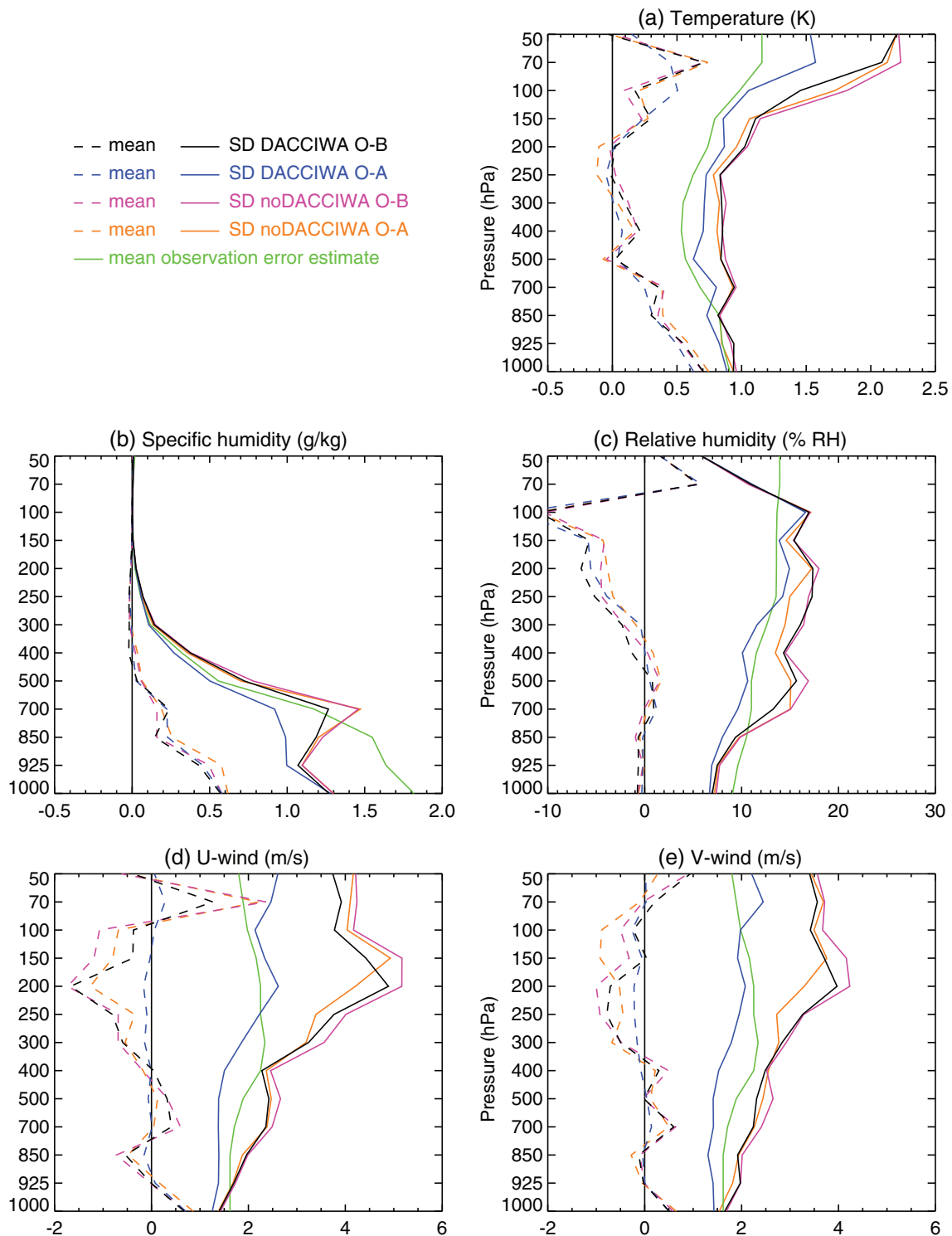


FIGURE 3 (a–e) Mean (dashed lines) and standard deviation (SD; solid lines) of differences between the radiosonde observations and the model background (O–B) and final analysis (O–A) for the DACCIWA and noDACCIWA experiments. Green lines show mean observation error estimate

can even be degraded. In contrast to temperature and humidity, the assimilation of DACCIWA wind measurements has an unmistakably positive impact on the bias, which is reduced to almost negligible values at all levels. Corrections are largest at the level of the 200 hPa tropical

easterly jet (TEJ) (Fink *et al.*, 2017). Consistent results are found for the standard deviation, which is reduced considerably for both components and all considered levels (blue solid lines in Figure 3d,e). Again, positive impacts of cycling and the assimilation of cloud-motion vectors are

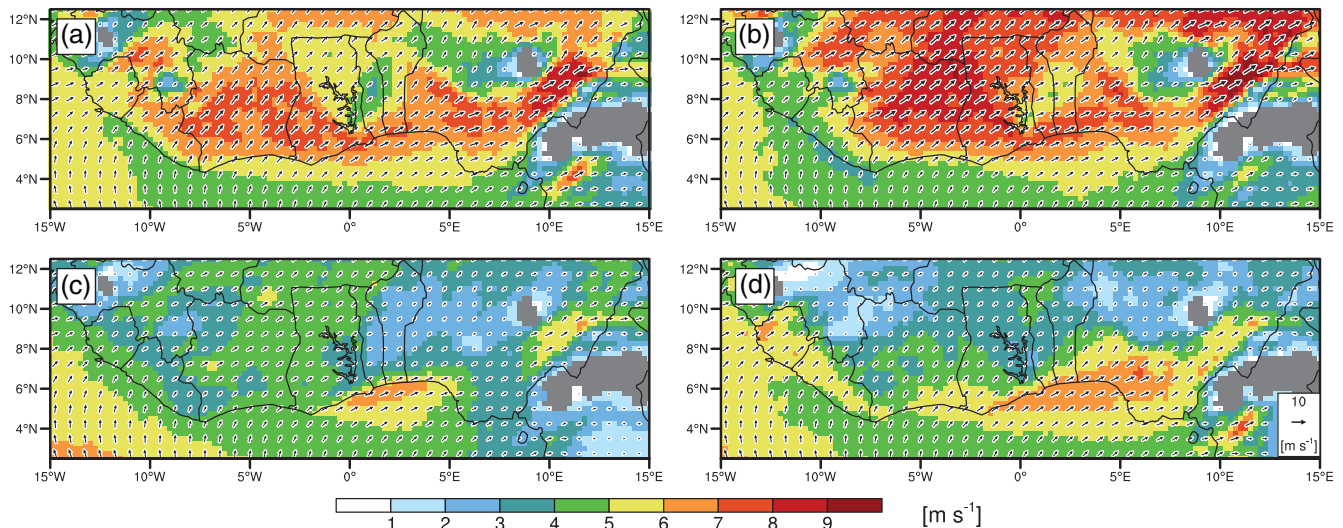


FIGURE 4 Mean 925 hPa wind speed (colours) and vectors at (a) 0000, (b) 0600, (c) 1200, and (d) 1800 UTC based on the DACCIWA analysis during 15 June to 31 July 2016. Only every third vector is shown. Regions where the 925 hPa pressure level lies below orography are masked in grey

evident at many levels. The green lines in Figure 3 show the mean observation error (or uncertainty) estimate used for these radiosondes. Some of the estimates seem about right, others seem to be too large, especially for low-level humidity.

Why is the impact of temperature and moisture data so small compared to wind measurements? Generally, the greater temporal and spatial variability of winds in the Tropics when compared to temperature and moisture should lead to smaller values in the background error covariance matrix and thus more weights to observations. The weak mass/wind balance in the Tropics leads to an effective decoupling between the impacts of temperature and wind measurements (e.g. Žagar *et al.*, 2008). Horizontal temperature gradients in the Tropics are very weak and thus the effective horizontal length-scales are long and even over West Africa might be affected by satellite observations over the oceans. This argument is weaker for humidity.

3.2 | Differences between DACCIWA and noDACCIWA analyses

This subsection discusses differences between the analyses with and without the assimilation of DACCIWA radiosondes, looking at horizontal maps over the entire DACCIWA region (and not just over the radiosonde locations as in Section 3.1). The results will be separated into differences with respect to winds (Section 3.2.1), temperature (Section 3.2.2), moisture (Section 3.2.3) and clouds (Section 3.2.4).

3.2.1 | Winds

Figure 4 shows the mean 925 hPa wind speed and vectors at 0000, 0600, 1200 and 1800 UTC (corresponds to local time in all DACCIWA countries except for Benin and Nigeria, where it is UTC + 1) based on the DACCIWA analyses averaged over the 47 days of the experiment. The low-level winds are predominantly southwesterly during all times, which agrees well with the mean July wind fields discussed by Fink *et al.* (2017). At 0000 UTC (Figure 4a) low-level winds are moderate over the ocean but show a clear acceleration inland with maxima over Ivory Coast, Ghana and southern Nigeria with indications of a channelling effect between the Jos Plateau and the mountains of the Cameroon Line (see Figure 1). A secondary maximum is evident in the Sahel in the far northern part of the figure. Until 0600 UTC (Figure 4b) winds accelerate markedly almost everywhere over land reaching values on the order of $10 \text{ m}\cdot\text{s}^{-1}$. The largest increases are seen over Mali where wind speeds almost double. There is also a mild tendency for a clockwise rotation of the wind between 0000 and 0600 UTC. This behaviour is indicative of the evolution of an NLLJ, which was already documented for the region by, for example, Knippertz *et al.* (2011) using radiosonde and reanalysis data. Previous studies have shown that the NLLJ plays an important role in the formation of low-level clouds over the study region (e.g. Schrage and Fink, 2012; Schuster *et al.*, 2013; Adler *et al.*, 2017). The extensive low-level cloud deck in turn was shown to strongly influence the short-wave radiation balance at the surface (Knippertz *et al.*, 2011; Hill *et al.*, 2018). This suggests that potential changes in low-level winds due to

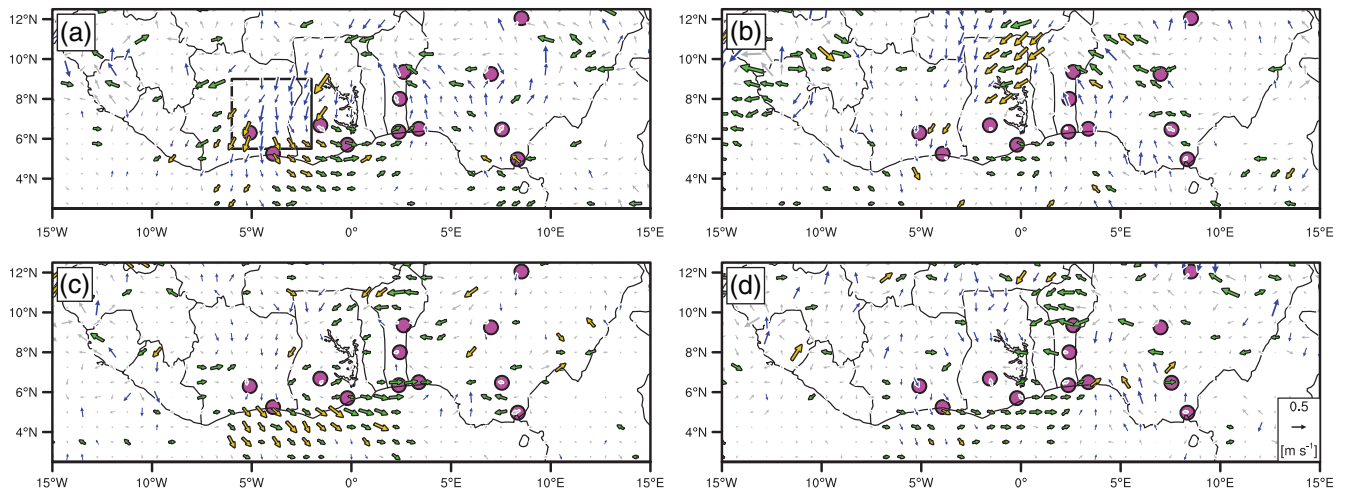


FIGURE 5 Influence of DACCIWA radiosonde data on low-level wind analysis. Mean differences of 925 hPa wind vectors between DACCIWA and noDACCIWA analysis at (a) 0000, (b) 0600, (c) 1200, and (d) 1800 UTC during 15 June to 31 July 2016. Only every third vector is shown. Colours of vectors indicate statistical significance of vector differences: blue vectors where only meridional component is significant, green vectors where only zonal component is significant, yellow vectors where both components are significant and grey vectors where no component is significant. Vectors in regions where the 925 hPa pressure level lies below orography are omitted. The black rectangle in (a) highlights the area for which the statistics in Figure 12a were calculated

the assimilation of radiosonde data might have important implications on other atmospheric fields. At 1200 UTC (Figure 4c) the wind speed markedly decreases everywhere over land as a consequence of the eddy drag caused by daytime turbulence in the PBL. Local maxima remain over the Bight of Benin and in the valley between the Jos Plateau and the Cameroon Line. Until 1800 UTC winds further decrease in the west to values around $4 \text{ m} \cdot \text{s}^{-1}$, while eastern areas, where the sunset is earlier, show first indications of NLLJ acceleration.

Figure 5 shows how the assimilation of DACCIWA radiosondes changes this diurnal wind pattern at 925 hPa. All times of day display coherent mean differences between the DACCIWA and noDACCIWA analyses peaking at approximately 5–10% relative to the mean wind speed (compare Figures 4 and 5), as well as some more scattered, noisy signals. The most prominent feature of the vector differences is a statistically significant reduction of southwesterly winds in the DACCIWA analyses mainly over Ivory Coast and Ghana at 0000 UTC (Figure 5a). The differences show a cyclonic pattern with westerlies off the coast of Ghana, Togo and Benin and (mostly non-significant) southerlies over Nigeria. At 0600 UTC the region with significant differences moves to northern parts of Ghana (Figure 5b), an area with strong acceleration in the absolute wind (Figure 4a,b). The cyclonic pattern in the difference is still evident. Assuming a positive impact of the additional observations as indicated by Figure 3d,e, these results suggest that the IFS overestimates the NLLJ acceleration above the weakly stable night-time PBL, particularly over flat terrain. Possible

reasons include issues with low-level cloud formation, shear-driven mixing or long-wave radiative cooling but a detailed analysis is beyond the scope of this article.

During the day (Figure 5c,d), significant biases are mostly restricted to the ocean, where they point to a possibly too strong monsoon flow in IFS. Over land, where winds are much weaker than during the night (Figure 4c,d), differences are predominantly weak and not significant, apart maybe from the easterlies over northern Benin. When averaged over all stations and times of day, the different signals cancel each other, leaving hardly any net difference at this level, consistent with the results for the radiosonde station locations shown in Figure 3d,e. Contrary to the data-denial experiments using AMMA radiosondes by Agustí-Panareda *et al.* (2010), no pronounced influence on the representation of the AEJ at 700 or 600 hPa can be identified (not shown). This is likely due to the more southern location of DACCIWA radiosonde stations, that is too far away from the AEJ axis over the Sahel.

For the level of the TEJ, that is, 200 hPa, however, the diurnal cycle is expectedly less pronounced than at 925 hPa (Figure 6) with a weak increase of the jet maximum over Ghana until 1200 UTC. Consistent with the reduction of O–A biases in zonal winds (Figure 3d), a large influence of DACCIWA radiosondes is found over and slightly south of the jet maximum at all times of day (Figure 7). Overall, the differences show an intensification of the TEJ but, especially over Ghana, the vectors do not only point westward but also in a southward direction. Combined with the overall increase in predicted precipitation to the north of this

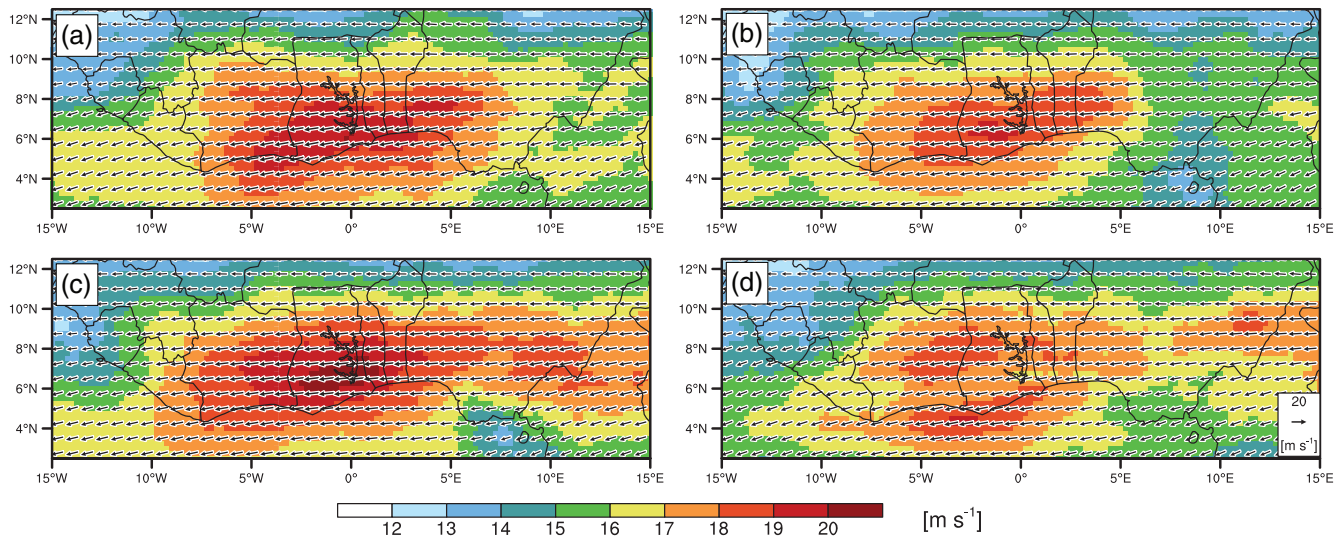


FIGURE 6 Same as in Figure 4 but for 200 hPa wind

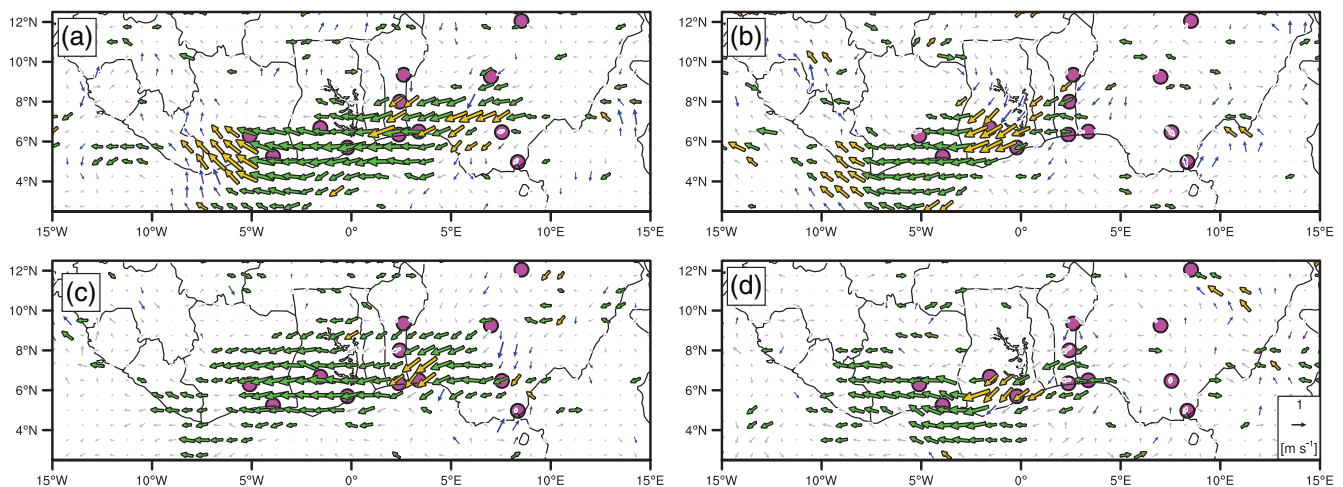


FIGURE 7 Same as in Figure 5 but for 200 hPa wind

area (Figure 14d), this may indicate an acceleration of the TEJ by divergent convective outflow as recently shown by Lemburg *et al.* (2019).

3.2.2 | Temperature

Figure 8 shows the corresponding analysis for mean 925 hPa temperature differences. As for low-level winds, values are most pronounced at 0000 and 0600 UTC (Figure 8a,b). At these times, the DACCIWA analyses are significantly warmer over most of Ivory Coast, Ghana, Togo and Benin as well as parts of adjacent countries and ocean areas, while cooler areas are almost absent. The mean differences peak at more than +0.4 K in the eastern and northeastern parts of Ivory Coast. This is in contrast to the relatively small bias reduction averaged over all

radiosonde stations, which only reaches just above 0.1 K (Figure 3a). It suggests that the differences we see in winds (Figure 5) likely have the main impact on the temperature differences through a reduction of cold air advection from the Gulf of Guinea and thus leading to higher temperatures downstream of the DACCIWA radiosonde locations. Changes in temperature can in turn affect the NLLJ via changes to stability. Through this mechanism, the temperature and wind signals can be coupled in a complicated, nonlinear way.

In contrast, temperature differences at 1200 and 1800 UTC (Figure 8c,d) are in general much weaker and more scattered. There is a certain tendency for southern areas in Ivory Coast and Ghana to be warmer in the DACCIWA analyses, while the Sahelian parts of the study region tend to be on the cold side. The latter could be attributed to an increase in the activity of organized convective systems

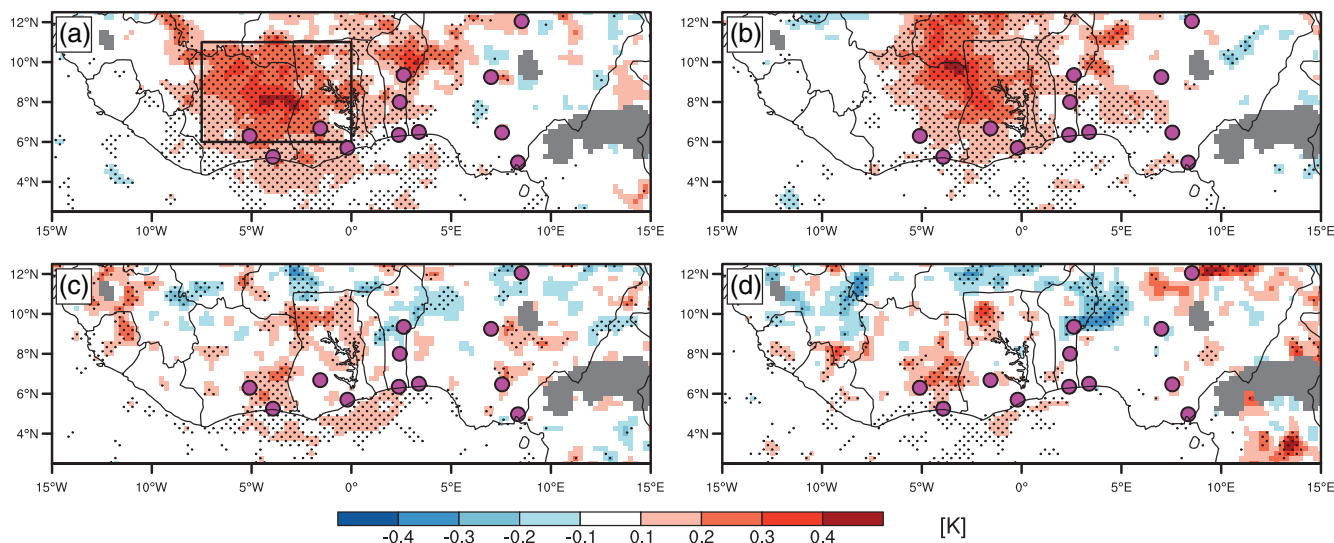


FIGURE 8 Influence of DACCIWA radiosonde data on low-level temperature analysis. Mean differences of 925 hPa temperature between DACCIWA and noDACCIWA analysis at (a) 0000, (b) 0600, (c) 1200, and (d) 1800 UTC during 15 June to 31 July 2016. Stippling highlights regions with statistically significant differences. Regions where the 925 hPa pressure level lies below orography are masked in grey. The black rectangle in (a) highlights the area for which the statistics in Figure 12b were calculated

(see also the precipitation changes in Figure 14d). The significant warm signal over the ocean at 1200 UTC is collocated with a weaker monsoon flow there (cf. Figure 5c). Both Figures 5 and 8 strongly suggest that the influence of DACCIWA radiosonde data is in general more important at 0000 and 0600 UTC, while strong daytime turbulent mixing in the PBL homogenises the lower atmosphere, creating smaller differences at 1200 and 1800 UTC (Kniffka *et al.*, 2019b). Therefore, the focus of the remaining part of this section will be on the 0000 and 0600 UTC analysis times.

One point to note is that – somewhat surprisingly – hardly any impact of DACCIWA radiosonde data on 2 m temperatures is discernible (not shown). One possible explanation is that the influence of radiosonde measurements would mostly be indirect through, for example, changes in temperature and moisture above 2 m height, cloudiness or the radiation balance.

3.2.3 | Moisture

Figure 9 provides a comparison of the influence of DACCIWA radiosonde data on low-level relative (top) and specific humidity (bottom) at 0000 and 0600 UTC, respectively. Since specific humidity analyses are only available on model levels, model level 120 was used as it is close to the 925 hPa pressure level. The results suggest that the differences of relative humidity are dominated by temperature, since the differences are mostly negative and occur in the regions with the highest positive

temperature differences, although the significant areas are much reduced (compare Figure 8a,b with Figure 9a,b). On the contrary, the differences in specific humidity (Figure 9c,d) show a more direct influence of the assimilation of radiosonde-measured humidity. Statistically significant differences in low-level specific humidity are mostly positive. Assuming an overall improvement through the assimilation of DACCIWA radiosondes, this would confirm the dry bias in the IFS already discussed in Section 3.1, particularly over Benin and southwestern Ghana. The reasons for this are not clear, as they are less strongly collocated with wind differences (Figure 5a,b). This suggests that issues with vertical mixing are more likely but these would then – somewhat surprisingly – only weakly impact temperature (Figure 8a,b). The dry bias is probably caused by forecast model deficiencies, but the data assimilation does nothing to reduce it in this area (Figure 3). The ECMWF analysis system has a nonlinear humidity transform that involves temperature as well (Hólm *et al.*, 2002). Ingleby *et al.* (2013) implemented a similar humidity transform in the Met Office system. In the current study the low-level temperature and humidity errors are positively correlated but the analysis results suggest that this is not well captured by the statistics used in the transform.

Looking at total column water vapour (TCWV), differences between the DACCIWA and noDACCIWA analyses display only a weak diurnal cycle in contrast to the other variables discussed so far (not shown). Therefore Figure 10 shows results for 0000 UTC as an example. For better orientation, Figure 10a first displays mean TCWV based on the DACCIWA analyses. Values range between

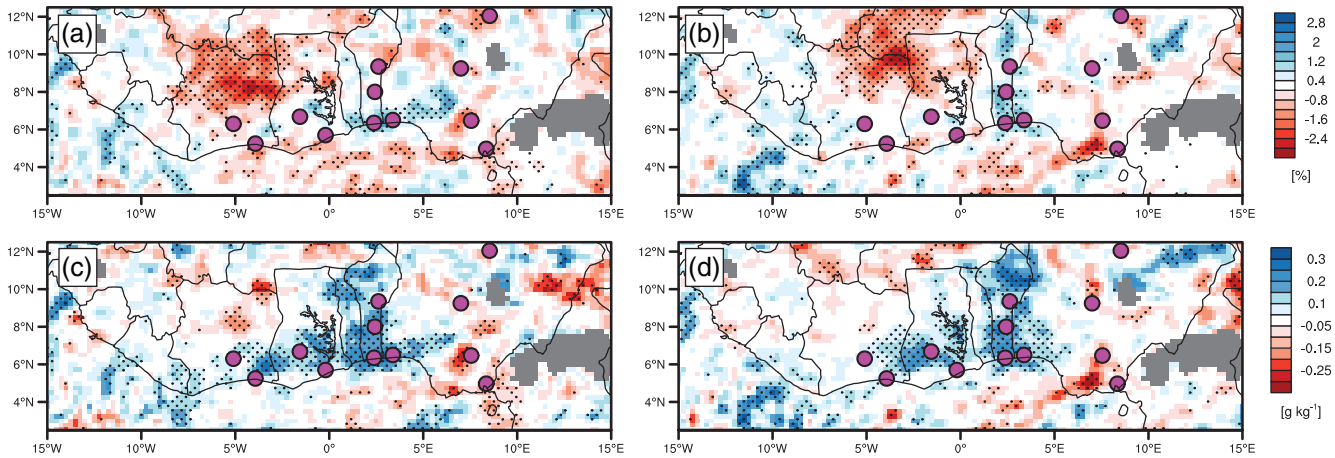
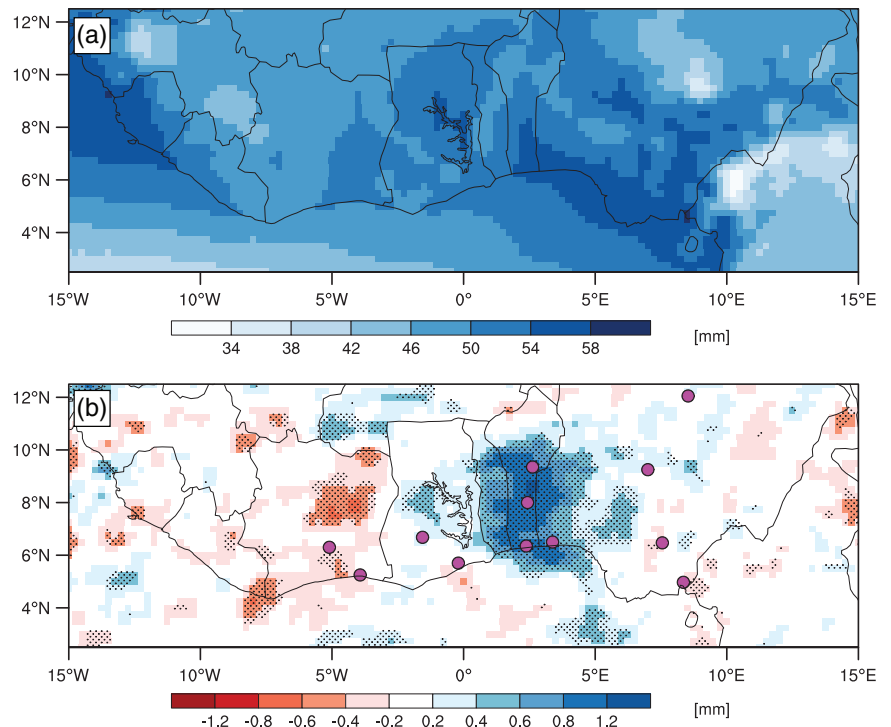


FIGURE 9 Influence of DACCIIWA radiosonde data on low-level moisture analysis. (a,b) Mean differences of 925 hPa relative humidity and (c,d) mean differences of specific humidity on model level 120 (near 925 hPa) between DACCIIWA and noDACCIIWA analysis at 0000 UTC (left column, a,c) and 0600 UTC (right column, b,d) during 15 June to 31 July 2016. Stippling highlights regions with statistically significant differences. Regions where the 925 hPa pressure level lies below orography are masked in grey

FIGURE 10 Influence of DACCIIWA radiosonde data on TCWV analysis. (a) Mean TCWV at 0000 UTC based on the DACCIIWA analysis and (b) mean differences of TCWV between DACCIIWA and noDACCIIWA analysis at 0000 UTC, during 15 June to 31 July 2016. Stippling in (b) highlights regions with statistically significant differences



about 34 mm over mountainous areas and around 55 mm along the wet coasts of Sierra Leone, Guinea and Nigeria (see Knippertz *et al.* (2017) for typical day-to-day variations during the campaign). Values around 50 mm are widespread over the continental lowlands. The differences between the two analyses (Figure 10b) are dominated by statistically significant positive values maximised over the three Beninese radiosonde stations with impacts spreading towards adjacent Togo, Nigeria and the Atlantic Ocean. Smaller significant patches are found over central Ghana and southwestern Burkina Faso. This is largely in good

agreement with the 925 hPa specific humidity differences shown in Figure 9c,d. Negative values are mostly restricted to several patches in and around Ivory Coast. Other times of day are similar with slightly weaker signals at 1200 and 1800 UTC (not shown).

3.2.4 | Clouds

Finally, Figure 11 shows the observation impact on cloud cover separated into high (top), medium (middle) and low

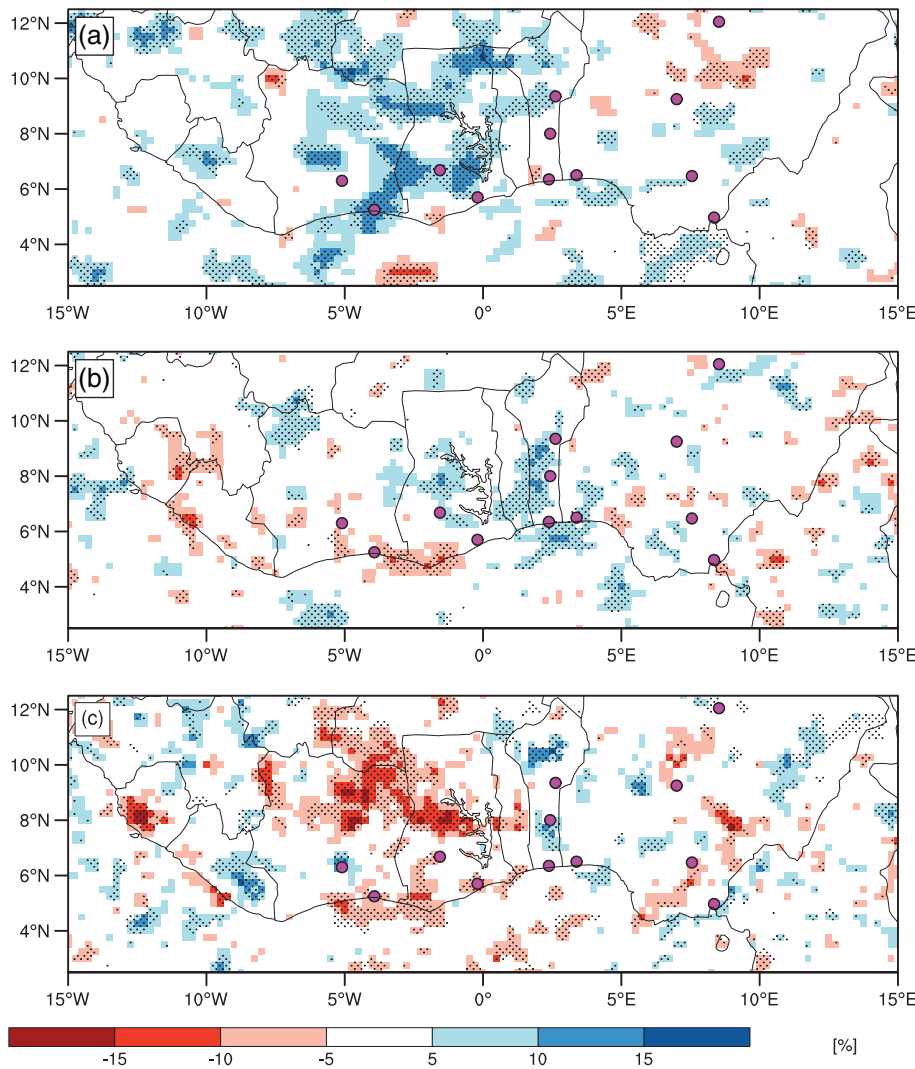


FIGURE 11 Influence of DACCIWA radiosonde data on cloud cover analysis. Mean differences of (a) high, (b) medium and (c) low cloud cover between DACCIWA and noDACCIWA analysis at 0600 UTC during 15 June to 31 July 2016. Stippling highlights regions with statistically significant differences

clouds (bottom). Here we concentrate on 0600 UTC when low-level cloud cover is close to its maximum (e.g. van der Linden *et al.*, 2015). Mean differences in medium cloud cover (Figure 11b) are weak at all times and only show a larger area of statistically significant differences over and around Benin, where also TCWV shows positive values (Figure 10b).

Signals in low clouds (Figure 11c) are considerably larger and more coherent. Assimilating DACCIWA observations reduces low-cloud cover by up to 15% in northern parts of Ivory Coast and central parts of Ghana. This suggests that the northward progression of the extensive nocturnal low-level cloud deck in this region (e.g. van der Linden *et al.*, 2015) is reduced when DACCIWA radiosonde data are assimilated. This is consistent with higher low-level temperatures (Figure 8b) and lower low-level relative humidity (Figure 9b), which, as explained above, may be partly attributed to weaker southwesterly advection in the course of the night (Figure 5a,b). The combination of less night-time cloud and warmer

temperatures underlines the fact that these clouds do not have a large impact on long-wave radiative cooling at the surface, because the very high TCWV (Figure 10a) alone suffices to suppress energy loss to higher levels (see figure 9c in Hill *et al.* (2018) and figure 4d in Kniffka *et al.* (2019b)). Differences are least pronounced at 1800 UTC (not shown), when the minimum cover of low cloud is reached over the study region (e.g. van der Linden *et al.*, 2015).

High-cloud cover in contrast is predominantly higher in the DACCIWA than in the noDACCIWA analyses (Figure 11a). The largest coherent regions with statistically significant differences occur over Ivory Coast, Ghana, Togo and Benin. Overall, the magnitude of the positive high-cloud cover differences is in a similar range as the magnitude of the negative low-cloud cover differences shown in Figure 11c. Over Nigeria, the differences are less pronounced and divided into positive values in the southern and negative values in the northern half of the country. The reason for this increase in high clouds is

not entirely clear but might be related to changes in deep convection and near-tropopause detrainment (see Figure 14d and the discussion of precipitation forecasts in Section 4). The signals are somewhat patchy but mostly occur in the vicinity of the big blob of higher low-level temperatures (Figure 8). Since the influence on temperatures on levels above 925 hPa is small (not shown), the higher low-level temperatures lead to slightly lower stability and thus potentially to an early triggering of convection. Overall, the influence on high-cloud cover is most pronounced at 0000 UTC (not shown), which coincides with the night-time maximum of high-cloud cover over the region as documented by Hill *et al.* (2016).

4 | INFLUENCE ON ECMWF FORECASTS

The purpose of this section is to investigate to what extent the observation impacts documented in Section 3 also impact on forecasts and whether this leads to an improvement when comparing to independent observations or the (supposedly superior) DACCIWA analysis data. While Section 4.1 concentrates on low-level temperature and wind, for which large impact was found in the analysis in Section 3.2, Sections 4.2 and 4.3 analyse impact on OLR and rainfall.

4.1 | Low-level wind and temperature

Figure 12 shows an evaluation of 925 hPa temperature and wind speed forecasts for different lead times. The evaluation is performed for all grid points in the areas that show the largest differences between the DACCIWA and noDACCIWA analyses of low-level wind vectors and temperature (i.e. black rectangles in Figures 5a and 8a). Solid lines show the DACCIWA forecasts, which start from an RMSE of zero, as the DACCIWA analyses are used for evaluation. Dashed lines show noDACCIWA forecasts with the RMSE at lead time zero reflecting the large differences documented in Figures 5 and 8. The colours then indicate different starting times, that is, 0000, 0600, 1200 and 1800 UTC. As pointed out already in Section 2, not all possible starting-time–lead-time pairs are available for this analysis.

With respect to wind speed (Figure 12a), RMSEs in noDACCIWA at lead-time zero range from 0.9 to 1 m s⁻¹ for all starting times. Error growth is then relatively flat reaching 1.55 m s⁻¹ for a 1200 UTC start and 2.0 m s⁻¹ for a 0000 UTC start after 48 hr. It is striking that for the

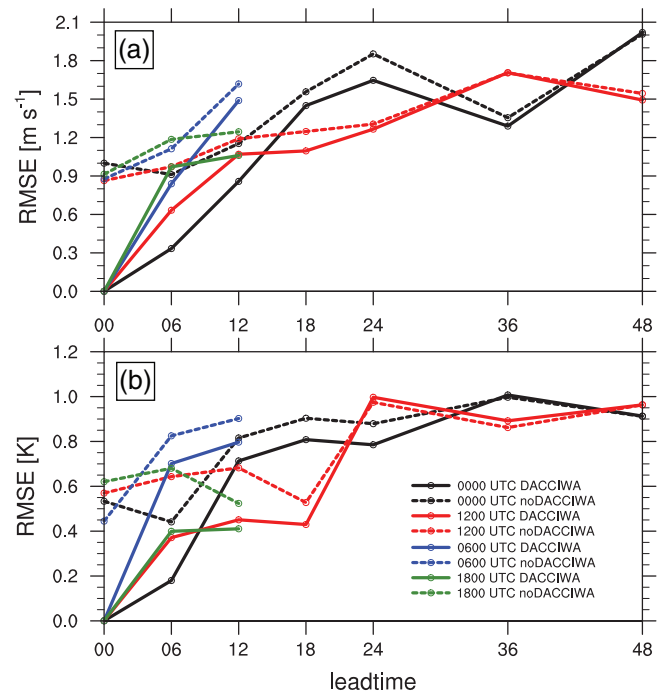


FIGURE 12 Influence of DACCIWA radiosonde data on low-level wind speed and temperature forecasts. RMSE of (a) 925 hPa wind speed and (b) 925 hPa temperature for different lead times (hr). The lines correspond to different forecast times for the DACCIWA and noDACCIWA forecasts. Calculations are based on the areas 5.5–9°N, 2–6°W for 925 hPa wind and 6–11°N, 0–7.5°W for 925 hPa temperature (cf. black rectangles in Figures 5a and 8a, respectively)

0000, 0600 and 1200 UTC runs there is a marked RMSE increase between 1200 and 1800 UTC, when the PBL grows deep and convection develops. This could be related to the previously documented fast error growth during small-scale convective processes (e.g. Selz and Craig, 2005; Zhang *et al.*, 2007; Žagar *et al.*, 2017; Judt, 2018) and indicates model issues with realistically handling the turbulent eddy drag and possibly growing local variability. In contrast to that, the DACCIWA runs show an abrupt increase in RMSE in the first forecast hours and almost catch up with the noDACCIWA runs after about 12 hr. The initial increase is smallest for the 0000 UTC run, when systematic differences between the two analyses are particularly large (Figure 5). As for the noDACCIWA runs, RMSE increases tend to be relatively large during daytime when strong turbulent mixing reduces the positive impact of DACCIWA radiosonde data, as already discussed for the analysis in Section 3.

The behaviour for temperature (Figure 12b) shows an overall similar pattern but initial RMSEs in noDACCIWA cover a larger range (0.45–0.62 K). Errors grow to about 0.9 K after 48 hr. The 0600 UTC forecast stands out as having the smallest initial RMSE (blue dashed line

in Figure 12b). As for wind speed, the positive impact of the observations vanishes largely in the first 12 hr of forecast. The RMSE stays lowest and the assimilation of DACCIWA observations maintains a positive impact out to 18 hr lead time when starting with improved nighttime temperatures, since at this time of day differences are largest (Figure 8a). These results clearly demonstrate that a combination of model error and chaotic behaviour, which depends to some extent on the time of day, makes it challenging to sustain a positive impact of additional observations beyond one diurnal cycle. This conclusion is largely consistent with Agusti-Panareda *et al.* (2010), who observed that the benefit of additional radiosonde data is almost absent after 24 hr of forecast.

4.2 | Outgoing long-wave radiation (OLR)

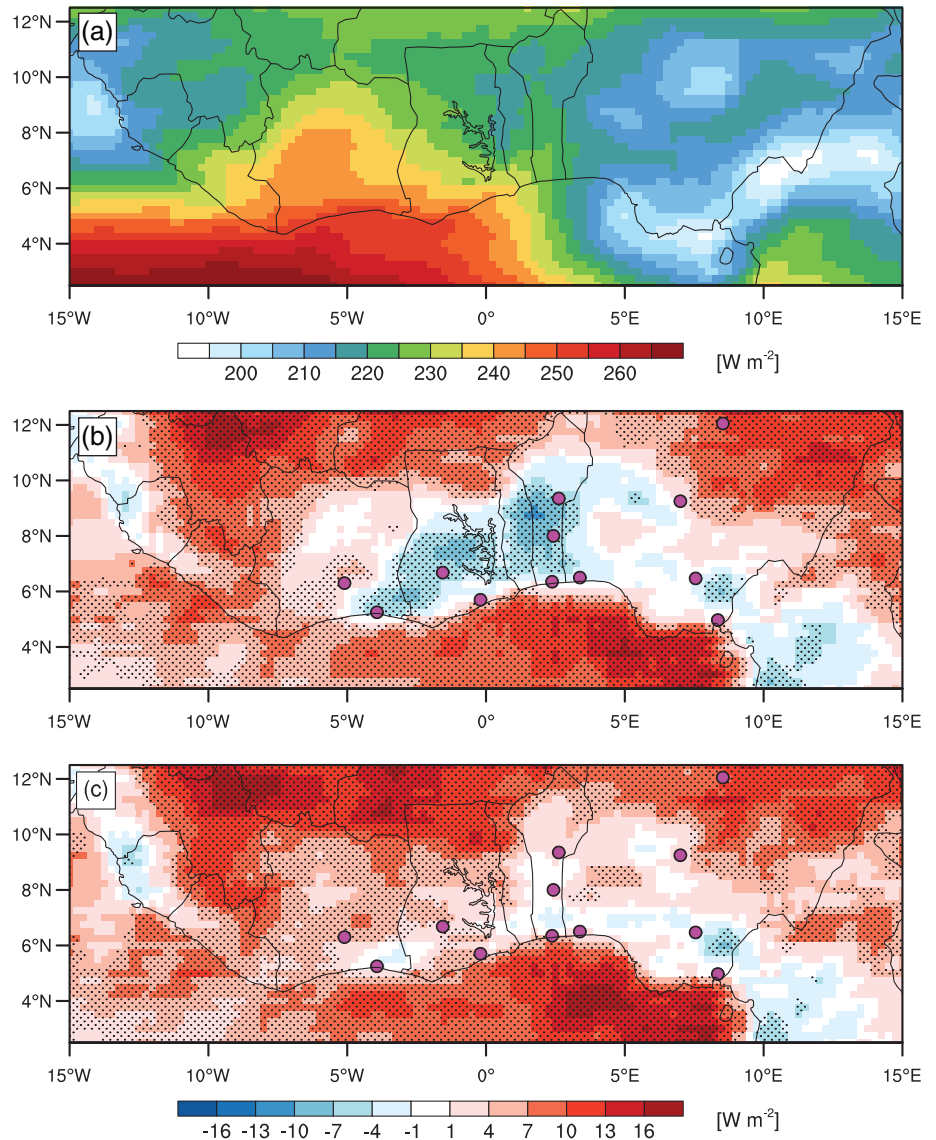
Figure 13 shows an evaluation of DACCIWA and noDACCIWA forecasts of mean daily OLR against the CM SAF TET dataset. The campaign average of the satellite dataset shows values varying from about 270 K over the dry equatorial Atlantic to less than 200 K off the coast of Guinea and Sierra Leone as well as over the Cameroon Line and around the Niger Delta, which highlights the frequent occurrence of deep convection. DACCIWA and noDACCIWA forecasts (Figure 13b,c) both show large positive biases of up to $16 \text{ W}\cdot\text{m}^{-2}$ over the eastern Gulf of Guinea and over the Sahel, indicating that the extent of deep convection over these regions is underestimated in both forecasts. While the extent and magnitude of these biases are similar over the western Sahel, positive biases over Burkina Faso and over some parts of the eastern Gulf of Guinea are reduced in DACCIWA forecasts compared to noDACCIWA forecasts. At the same time, however, the assimilation of DACCIWA radiosonde data leads to negative biases of TOA OLR over parts of Ghana, Togo and Benin, making the forecast worse in parts of this area. One possible explanation for this is that convection is too easily initiated here due to the higher amount of moisture in the atmospheric column (Figure 10b). However, the negative biases are not necessarily only a result of enhanced deep convection over this region, but are also influenced by the higher amount of TCWV detected in the DACCIWA analyses (Figure 10b). Using $t + 36$ hr and $t + 12$ hr forecasts instead of $t + 24$ hr and $t + 0$ hr forecasts leads to a much greater similarity of biases in both the DACCIWA and noDACCIWA forecasts (not shown). This suggests that the impact of additional radiosonde data on OLR forecasts strongly decreases already within the first 12 hr of the forecasts.

4.3 | Precipitation

Figure 14 shows a corresponding analysis for mean daily rainfall. The observational dataset CHIRPS 2.0, which is only available over land, reveals rainfall maxima at the coasts of Guinea, Sierra Leone and near the Niger Delta (Figure 14a), which agrees well with the overall patterns of OLR minima (Figure 13a). The biases of the DACCIWA (Figure 14b) and noDACCIWA forecasts (Figure 14c) relative to CHIRPS 2.0 are overall quite similar. IFS has a wet bias in the coastal zones of eastern Ivory Coast to western Nigeria, over western Guinea and central Cameroon, while the Sahel tends to have a negative bias, most pronounced in the border area of northeastern Nigeria and Cameroon. The very localised and large dry biases along the west coast of West Africa may be caused by an inability of the model to resolve coastal circulations. However, the dry biases could also indicate a problem of CHIRPS 2.0 to deal with the sharp gradients along the coast in the precipitation retrieval. More moderate dry biases are found over the adjacent Guinea Highlands, which are possibly not sufficiently represented in the IFS model due to the employed grid spacing of 0.25° . Consistently for both experiments, regional maxima of wet biases occur a bit inland from the coasts that could be related to the occurrence of convection related to the sea-breeze circulation (e.g. Guedje *et al.*, 2019).

Comparing the biases between the two forecasts in the area of dense radiosonde observations reveals a mild improvement, mostly downstream over central Ivory Coast, Burkina Faso and Mali. Recall that $+12$ to $+36$ hr forecasts are analysed here such that there is enough time for a given observation impact to propagate downstream with the monsoon flow. The results just discussed are relatively independent of the choice of observational dataset, since using the final daily $0.1^\circ \times 0.1^\circ$ Global Precipitation Measurement Mission Integrated Multi-Satellite Retrievals for GPM (GPM IMERG) V06B dataset (Huffman *et al.*, 2019) as a reference for calculating the biases does not change much (not shown). To bring out the impact of the additional observations a little more clearly, Figure 14d shows the mean differences of daily precipitation between the DACCIWA and noDACCIWA forecasts. Although the differences are generally noisy and often not statistically significant, there is a region with predominantly positive differences stretching from southwestern Nigeria across southern Benin and northeastern Ghana into Burkina Faso and Mali. The northern part of this region coincides with the area of increased upper-level clouds in the DACCIWA analysis (Figure 11a). West-southwestward advection with the predominant flow at the TEJ level (cf. Figure 6) may have helped spread cirrus clouds into southwestern parts of Ghana and adjacent Ivory Coast.

FIGURE 13 Influence of DACCIWA radiosonde data on TOA OLR forecasts. (a) Mean daily OLR based on CMSAF TET data and biases of (b) DACCIWA and (c) noDACCIWA forecasts with respect to CMSAF TET data, during 15 June to 31 July 2016. Stippling in (b) and (c) highlights regions with statistically significant biases



5 | CONCLUSIONS

Accurate weather forecasts have a high potential for socio-economic benefit in densely populated southern West Africa, but current operational systems are not able to provide guidance of sufficient quality. A central question in this context is whether the deficiencies are mostly a result of inadequate models and data assimilation systems or insufficient observations. Data-denial experiments are a powerful tool to investigate this question. Data assimilation and forecasting in the Tropics present different challenges to midlatitude prediction and – with the exception of tropical cyclones – these challenges have received relatively little attention. The unprecedented dataset of about 900 radiosonde measurements from 12 stations in southern West Africa gathered during the DACCIWA field campaign in June–July 2016 (Flamant *et al.*, 2018) provides a unique opportunity to evaluate how

these additional observations influence the quality of the ECMWF analyses and subsequent forecasts by running the IFS with and without assimilating these data. The results help identify the most promising avenues to future forecast improvement. The main conclusions from these data-denial experiments are as follows:

- Short-range forecasts with the IFS are too cold and too dry at low levels over southern West Africa. A similar temperature bias is seen more widely in the Tropics (Ingleby, 2017). Unfortunately, the assimilation of the additional radiosonde measurements does very little to reduce these biases, while corrections to wind biases are effective throughout the troposphere and lower stratosphere. The standard deviation of observation–analysis differences are reduced for all parameters and all levels but again impacts on winds are largest. This result is likely due to the little day-to-day

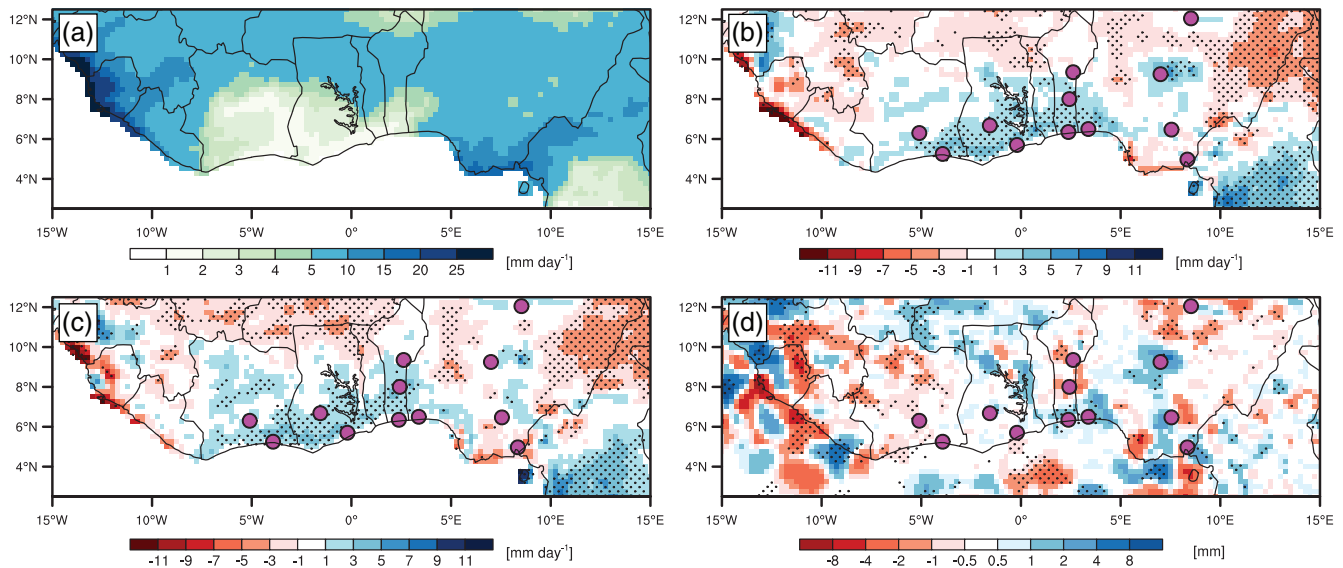


FIGURE 14 Influence of DACCIWA radiosonde data on rainfall forecasts. (a) Mean daily rainfall based on CHIRPS 2.0 data, biases of (b) DACCIWA and (c) noDACCIWA forecasts with respect to CHIRPS 2.0 data and (d) mean difference of daily rainfall forecasts between DACCIWA and noDACCIWA, during 15 June to 31 July 2016. Stippling in (b), (c), and (d) highlights regions with statistically significant biases/differences

variability of temperature and its very long horizontal error correlation scales (e.g. Ingleby, 2001), leading to a low weight for observations in the analysis process. These results also confirm the particular importance of wind assimilation in the Tropics (Žagar *et al.*, 2008; Stoffelen *et al.*, 2005; Baker *et al.*, 2014).

- DACCIWA radiosonde data have a considerable influence on low-level wind and temperature analyses to the north (i.e. downstream relative to the monsoon flow) of the radiosonde stations, mostly over the lowland parts of Ivory Coast and Ghana. In DACCIWA analyses (i.e. containing the additional observations), weaker cold air advection from the Gulf of Guinea due to weaker low-level southwesterly winds during the second half of the night appear to cause higher low-level temperatures, which reduce low-level relative humidity and cloud cover. Benin and parts of adjacent countries show an increase in low-level specific humidity and TCWV when assimilating the DACCIWA radiosondes. The influence of radiosonde data in low levels is generally most pronounced at night and in the early morning, while strong turbulent mixing in the daytime PBL appears to reduce the observation impact.
- The inclusion of DACCIWA radiosonde data leads to enhanced high-level cloud cover over parts of the study region, possibly related to more deep convection, and to an acceleration of the TEJ.
- With respect to forecast improvement, a positive impact of DACCIWA radiosonde data on low-level wind and temperature predictions does not extend beyond

12–24 hr lead time, with details depending on the time of day.

- Forecasts of OLR and rainfall show large and significant biases when compared to independent satellite measurements, including an underestimation of rainfall (and thus too warm OLR) over the Sahel and overestimation of rainfall near the Guinea Coast (i.e. where the DACCIWA radiosonde stations are located). Assimilation of the additional radiosonde data is not able to cure these problems. While observation impacts on OLR are somewhat ambiguous, there is a weak but robust improvement in rainfall forecasts downstream (i.e. to the north) of the DACCIWA radiosonde stations.

In interpreting these results, one should keep in mind the limited availability of data. The evaluation was only made for 47 days, that is, the length of the radiosonde campaign, and there are spatial and temporal differences in the number of available measurements (cf. Table 1). Despite this, all results discussed above are statistically significant at the 5% level and mostly coherent over a larger spatial area.

The results presented here demonstrate that more than 10 years after the AMMA field campaign and the associated data-denial experiments by Agustí-Panareda *et al.* (2010) the benefit of additional radiosonde data on ECMWF forecasts remains marginal and restricted to short-term forecasts of about 1–2 days. Together with the relatively large errors found already in the analysis data, this suggests that the main limiting factors for better

forecasts over southern West Africa are model errors and issues with the data assimilation system. It has recently been shown that tropical low-level humidity biases in the IFS are increased by the assimilation of satellite soundings (although these help to reduce random errors: Bormann *et al.*, 2019) and that the low vertical resolution of the satellite information causes challenges for the assimilation system. These issues are an area for future work.

Largest observation impact during the night point to problems with the weakly stable nocturnal PBL, while marked increases in forecast errors during the day indicate issues, when turbulence and convection are more active. Another possible source of errors is the parametrization of convection. Negative OLR biases in a region where TCWV values are higher in the DACCIWA analyses (compare Figures 13 and 10) suggests that convection may be triggered too easily in the IFS or is too sensitive to the amount of atmospheric moisture. The notion that model errors are an important source of bias is supported by the fact that the differences found in the more recent DACCIWA data-denial experiments are generally smaller than those in the older AMMA experiments (compare, e.g., figure 7b from Agustí-Panareda *et al.* (2010) and Figure 8). Interestingly, the present study finds a deceleration of the low-level monsoonal winds at the Guinea Coast, while Agustí-Panareda *et al.* (2010) found a strengthening of the low-level southwesterlies by assimilating radiosonde data. While Tompkins *et al.* (2005) and Agustí-Panareda *et al.* (2010) stated that the assimilation of radiosonde measurements is important to correctly represent the AEJ in the IFS, the present study documented a similar positive impact on the TEJ.

Ultimately more efforts are needed to investigate in much more detail the model errors in the IFS over a meteorological complicated region such as summertime West Africa. Although the additional observations taken during DACCIWA do not lead to a large forecast improvement *per se*, they still offer an important observational benchmark that can be employed for model development. Particularly, aspects of low-level meteorological fields and their diurnal behaviour were documented in much detail by the ground-based measurements of DACCIWA (Kalthoff *et al.*, 2018) that have already led to a comprehensive new conceptual model for low-cloud formation and dissolution (Lohou *et al.*, 2020). A further reduction of model errors in the IFS would not only be beneficial for the affected tropical regions, but could also improve forecasts in the extratropics, as shown by, for example, Žagar *et al.* (2015), Dias and Kiladis (2019) and Pante and Knippertz (2019).

ACKNOWLEDGEMENTS


The DACCIWA project has received funding from the European Union Seventh Framework Programme

(FP7/2007-2013) under grant agreement no. 603502. At ECMWF the support of Ioannis Mallas, who helped in the processing of the radiosonde data not received in real-time, is acknowledged. We would like to thank two anonymous reviewers for their valuable comments that helped to improve the manuscript


ORCID


Roderick van der Linden  <https://orcid.org/0000-0002-7364-323X>

Peter Knippertz  <https://orcid.org/0000-0001-9856-619X>

Andreas H. Fink  <https://orcid.org/0000-0002-5840-2120>

Bruce Ingleby  <https://orcid.org/0000-0002-3410-3951>

Marlon Maranan  <https://orcid.org/0000-0002-0324-8859>

Angela Benedetti  <https://orcid.org/0000-0002-9971-9976>

REFERENCES

- Adler, B., Kalthoff, N. and Gantner, L. (2017) Nocturnal low-level clouds over southern West Africa analysed using high-resolution simulations. *Atmospheric Chemistry and Physics*, 17, 899–910. <https://doi.org/10.5194/acp-17-899-2017>.
- Adler, B., Babić, K., Kalthoff, N., Lohou, F., Lohou, M., Dione, C., Pedruzo-Bagazgoitia, X. and Andersen, H. (2019) Nocturnal low-level clouds in the atmospheric boundary layer over southern West Africa: an observation-based analysis of conditions and processes. *Atmospheric Chemistry and Physics*, 19, 663–681. <https://doi.org/10.5194/acp-19-663-2019>.
- Agustí-Panareda, A., Vasiljevic, D., Beljaars, A., Bock, O., Guichard, F., Nuret, M., Garcia Mendez, A., Andersson, E., Bechtold, P., Fink, A., Hersbach, H., Lafore, J.-P., Ngamini, J.-B., Parker, D.J., Redelsperger, J.-L. and Tompkins, A.M. (2009) Radiosonde humidity bias correction over the West African region for the special AMMA reanalysis at ECMWF. *Quarterly Journal of the Royal Meteorological Society*, 135, 595–617. <https://doi.org/10.1002/qj.396>.
- Agustí-Panareda, A., Beljaars, A., Cardinali, C., Genkova, I. and Thorncroft, C. (2010) Impacts of assimilating AMMA soundings on ECMWF analyses and forecasts. *Weather and Forecasting*, 25, 1142–1160. <https://doi.org/10.1175/2010WAF2222370.1>.
- Andersson, E. and Thépaut, J.-N. (2008) *ECMWF's 4D-Var data assimilation system – the genesis and ten years in operations*. *ECMWF Newsletter*, 115, 8–12. <https://doi.org/10.21957/wnmguimihe>.
- Baker, W.E., Atlas, R., Cardinali, C., Clement, A., Emmitt, G.D., Gentry, B.M., Hardesty, R.M., Källén, E., Kavaya, M.J., Langland, R., Ma, Z., Masutani, M., McCarty, W., Pierce, R.B., Pu, Z., Riishojgaard, L.P., Ryan, J., Tucker, S., Weissmann, M. and Yoe, J.G. (2014) Lidar-measured wind profiles: the missing link in the global observing system. *Bulletin of the American Meteorological Society*, 95, 543–564. <https://doi.org/10.1175/BAMS-D-12-00164.1>.
- Bechtold, P., Semane, N., Lopez, P., Chaboureaud, J.-P., Beljaars, A. and Bormann, N. (2014) Representing equilibrium and non-equilibrium convection in large-scale models. *Journal of the*

- Atmospheric Sciences*, 71, 734–753. <https://doi.org/10.1175/JAS-D-13-0163.1>.
- Birch, C.E., Parker, D.J., Marsham, J.H., Copsey, D. and Garcia-Carreras, L. (2014) A seamless assessment of the role of convection in the water cycle of the West African monsoon. *Journal of Geophysical Research: Atmospheres*, 119, 2890–2912. <https://doi.org/10.1002/2013JD020887>.
- Bormann, N., Lawrence, H. and Farnan, J. (2019) *Global observing system experiments in the ECMWF assimilation system*. ECMWF Technical Memorandum, 839, 1–24. <https://doi.org/10.21957/sr184iyz>.
- Bougeault, P., Toth, Z., Bishop, C., Brown, B., Burridge, D., Chen, D.H., Ebert, B., Fuentes, M., Hamill, T.M., Mylne, K., Nicolau, J., Paccagnella, T., Park, Y.-Y., Parsons, D., Raoult, B., Schuster, D., Dias, P.S., Swinbank, R., Takeuchi, Y., Tennant, W., Wilson, L. and Worley, S. (2010) The THORPEX interactive grand global ensemble. *Bulletin of the American Meteorological Society*, 91, 1059–1072. <https://doi.org/10.1175/2010BAMS2853.1>.
- Couvreux, F., Guichard, F., Gounou, A., Bouniol, D., Peyrill e, P. and K ohler, M. (2014) Modelling of the thermodynamical diurnal cycle in the lower atmosphere: a joint evaluation of four contrasted regimes in the Tropics over land. *Boundary-Layer Meteorology*, 150, 185–214. <https://doi.org/10.1007/s10546-013-9862-6>.
- Dezfuli, A.K., Ichoku, C.M., Mohr, K. and Huffman, G.J. (2017) Precipitation characteristics in West and East Africa, from satellite and *in-situ* observations. *Journal of Hydrometeorology*, 18, 1799–1805. <https://doi.org/10.1175/JHM-D-17-0068.1>.
- Dias, J. and Kiladis, G.N. (2019) The influence of tropical forecast errors on higher latitude predictions. *Geophysical Research Letters*, 46, 4450–4459. <https://doi.org/10.1029/2019GL082812>.
- Dione, C., Lohou, F., Lothon, M., Adler, B., Babi c, K., Kalthoff, N., Pedruzo-Bagazgoitia, X., Bezombes, Y. and Gabella, O. (2019) Low-level stratiform clouds and dynamical features observed within the southern West African monsoon. *Atmospheric Chemistry and Physics*, 19, 8979–8997. <https://doi.org/10.5194/acp-19-8979-2019>.
- Druryan, L.M., Feng, J., Cook, K.H., Xue, Y., Fulakeza, M., Hagos, S.M., Konar e, A., Moufama-Okia, W., Powell, D.P., Vizy, E.K. and Ibrah, S.S. (2010) The WAMME regional model intercomparison study. *Climate Dynamics*, 35, 175–192. <https://doi.org/10.1007/s00382-009-0676-7>.
- Engel, T., Fink, A.H., Knippertz, P., Pante, G. and Bliedernicht, J. (2017) Extreme precipitation in the West African cities of Dakar and Ouagadougou – atmospheric dynamics and implications for flood risk assessments. *Journal of Hydrometeorology*, 18, 2937–2957. <https://doi.org/10.1175/JHM-D-16-0218.1>.
- EUMETSAT. (2019) *CM SAF TET - Emitted thermal radiative flux at top of atmosphere, product version 303*. Available at: <https://wui.cmsaf.eu/safira/> [Accessed 10 December 2019].
- Faccani, C., Rabier, F., Fourri e, N., Agusti-Panareda, A., Karbou, F., Moll, P., Lafore, J., Nuret, M., Hdidou, F. and Bock, O. (2009) The impacts of AMMA radiosonde data on the French global assimilation and forecast system. *Weather and Forecasting*, 24, 1268–1286. <https://doi.org/10.1175/2009WAF2222237.1>.
- Fink, A.H., Engel, T., Ermert, V., van der Linden, R., Schneidewind, M., Redl, R., Afiesimama, E., Thiaw, W.M., Yorke, C., Evans, M. and Janicot, S. (2017) *Mean climate and seasonal cycle*. *Meteorology of Tropical West Africa: The Forecasters' Handbook*. Chichester, UK: John Wiley & Sons, pp. 1–39.
- Flamant, C., Knippertz, P., Fink, A.H., Akpo, A., Brooks, B., Chiu, C.J., Coe, H., Danuor, S., Evans, M., Jegede, O., Kalthoff, N., Konar e, A., Lioussse, C., Lohou, F., Mari, C., Schlager, H., Schwarzenboeck, A., Adler, B., Amekudzi, L., Aryee, J., Ayoola, M., Batenburg, A.M., Bessardon, G., Borrmann, S., Brito, J., Bower, K., Burnet, F., Catoire, V., Colomb, A., Denjean, C., Fosu-Amankwah, K., Hill, P.G., Lee, J., Lothon, M., Maranan, M., Marsham, J., Meynadier, R., Ngamini, J., Rosenberg, P., Sauer, D., Smith, V., Stratmann, G., Taylor, J.W., Voigt, C. and Yobou e, V. (2018) The Dynamics–Aerosol–Chemistry–Cloud Interactions in West Africa field campaign: overview and research highlights. *Bulletin of the American Meteorological Society*, 99, 83–104. <https://doi.org/10.1175/BAMS-D-16-0256.1>.
- Funk, C., Peterson, P., Landsfeld, M., Pedreros, D., Verdin, J., Shukla, S., Husak, G., Rowland, J., Harrison, L., Hoell, A. and Michaelsen, J. (2015) The climate hazards infrared precipitation with stations – a new environmental record for monitoring extremes. *Scientific Data*, 2(1), 150066. <https://doi.org/10.1038/sdata.2015.66>.
- Guedje, F.K., Houeto, A.V.V., Houngninou, E.B., Fink, A.H. and Knippertz, P. (2019) Climatology of coastal wind regimes in Benin. *Meteorologische Zeitschrift*, 28, 23–39. <https://dx.doi.org/10.1127/metz/2019/0930>.
- Hannak, L., Knippertz, P., Fink, A.H., Kniffka, A. and Pante, G. (2017) Why do global climate models struggle to represent low-level clouds in the West African summer monsoon? *Journal of Climate*, 30, 1665–1687. <https://doi.org/10.1175/JCLI-D-16-0451.1>.
- Hill, P.G., Allan, R.P., Chiu, J.C. and Stein, T.H.M. (2016) A multisatellite climatology of clouds, radiation, and precipitation in southern West Africa and comparison to climate models. *Journal of Geophysical Research: Atmospheres*, 121, 10857–10879. <https://doi.org/10.1002/2016JD025246>.
- Hill, P.G., Allan, R.P., Chiu, J.C., Bodas-Salcedo, A. and Knippertz, P. (2018) Quantifying the contribution of different cloud types to the radiation budget in southern West Africa. *Journal of Climate*, 31, 5273–5291. <https://doi.org/10.1175/JCLI-D-17-0586.1>.
- H olm, E., Andersson, E., Beljaars, A., Lopez, P., Mahfouf, J.-F., Simons, A.J. and Th epaut, J.-N. (2002) *Assimilation and modelling of the hydrological cycle: ECMWF's status and plans*. ECMWF Technical Memorandum, 383, 1–55. <https://doi.org/10.21957/kry8prwuq>.
- Huffman, G.J., Stocker, E.F., Bolvin, D.T., Nelkin, E.J. and Tan, J. (2019) *GPM IMERG Final Precipitation L3 1 day 0.1 degree x 0.1 degree V06*. *Greenbelt, MD: Goddard Earth Sciences Data and Information Services Center (GES DISC)*. <https://doi.org/10.5067/GPM/IMERGDF/DAY/06>.
- Ingleby, N.B. (2001) The statistical structure of forecast errors and its representation in The Met. Office Global 3-D Variational Data Assimilation Scheme. *Quarterly Journal of the Royal Meteorological Society*, 127, 209–231. <https://doi.org/10.1002/qj.49712757112>.
- Ingleby, N.B. (2017) *An assessment of different radiosonde types 2015/2016*. ECMWF Technical Memorandum 807.
- Ingleby, N.B., Lorenc, A.C., Ngan, K., Rawlins, F. and Jackson, D.R. (2013) Improved variational analyses using a nonlinear humidity control variable. *Quarterly Journal of the Royal Meteorological Society*, 139, 1875–1887. <https://doi.org/10.1002/qj.2073>.
- Judt, F. (2018) Insights into atmospheric predictability through global convection-permitting model simulations. *Journal of the*

- Atmospheric Sciences*, 75, 1477–1497. <https://doi.org/10.1175/JAS-D-17-0343.1>.
- Kalthoff, N., Lohou, F., Brooks, B., Jegede, G., Adler, B., Babic, K., Dione, C., Ajao, A., Amekudzi, L.K., Aryee, J.N.A., Ayoola, M., Bessardon, G., Danuor, S.K., Handwerker, J., Kohler, M., Lothon, M., Pedruzo-Bagazgoitia, X., Smith, V., Sunmonu, L., Wieser, A., Fink, A.H. and Knippertz, P. (2018) An overview of the diurnal cycle of the atmospheric boundary layer during the West African monsoon season: results from the 2016 observational campaign. *Atmospheric Chemistry and Physics*, 18, 2913–2928. <https://doi.org/10.5194/acp-18-2913-2018>.
- Karbou, F., Rabier, F., Lafore, J.-P., Redelsperger, J.-L. and Bock, O. (2010) Global 4DVAR assimilation and forecast experiments using AMSU observations over land. Part II: Impacts of assimilating surface-sensitive channels on the African monsoon during AMMA. *Weather and Forecasting*, 25, 20–36. <https://doi.org/10.1175/2009WAF2222244.1>.
- Kelly, G., Thépaut, J.-N., Buizza, R. and Cardinali, C. (2007) The value of observations. I: Data denial experiments for the Atlantic and the Pacific. *Quarterly Journal of the Royal Meteorological Society*, 133, 1803–1815. <https://doi.org/10.1002/qj.150>.
- Kniffka, A., Knippertz, P., Fink, A.H., Benedetti, A., Brooks, M.E., Hill, P.G., Maranan, M., Pante, G. and Vogel, B. (2019a) An evaluation of operational and research weather forecasts for southern West Africa using observations from the DACCWA field campaign in June–July 2016. *Quarterly Journal of the Royal Meteorological Society*, 1–28. <https://doi.org/10.1002/qj.3729>.
- Kniffka, A., Knippertz, P. and Fink, A.H. (2019b) The role of low-level clouds in the West African monsoon system. *Atmospheric Chemistry and Physics*, 19, 1623–1647. <https://doi.org/10.5194/acp-19-1623-2019>.
- Knippertz, P., Fink, A.H., Schuster, R., Trentmann, J., Schrage, J.M. and Yorke, C. (2011) Ultra-low clouds over the southern West African monsoon region. *Geophysical Research Letters*, 38, L21808. <https://doi.org/10.1029/2011GL049278>.
- Knippertz, P., Coe, H., Chiu, J.C., Evans, M.J., Fink, A.H., Kalthoff, N., Lioussé, C., Mari, C., Allan, R.P., Brooks, B., Danour, S., Flamant, C., Jegede, O.O., Lohou, F. and Marsham, J.H. (2015) The DACCWA project: Dynamics–Aerosol–Chemistry–Cloud Interactions in West Africa. *Bulletin of the American Meteorological Society*, 96, 1451–1460. <https://doi.org/10.1175/BAMS-D-14-00108.1>.
- Knippertz, P., Fink, A.H., Deroubaix, A., Morris, E., Tocquer, F., Evans, M.J., Flamant, C., Gaetani, M., Lavaysse, C., Mari, C., Marsham, J.H., Meynadier, R., Affo-Dogo, A., Bahaga, T., Brosse, F., Deetz, K., Guebsi, R., Latifou, I., Maranan, M., Rosenberg, P.D. and Schlueter, A. (2017) A meteorological and chemical overview of the DACCWA field campaign in West Africa in June–July 2016. *Atmospheric Chemistry and Physics*, 17, 10893–10918. <https://doi.org/10.5194/acp-17-10893-2017>.
- Kouadio, K., Bastin, S., Konare, A. and Ajayi, V.O. (2018) Does convection-permitting simulate better rainfall distribution and extreme over Guinean coast and surroundings? *Climate Dynamics*, 1–22. <https://doi.org/10.1007/s00382-018-4308-y>.
- Lafore, J.-P., Flamant, C., Guichard, F., Parker, D.J., Bouniol, D., Fink, A.H., Giraud, V., Gosset, M., Hall, N., Höller, H., Jones, S.C., Protat, A., Roca, R., Roux, F., Saïd, F. and Thorncroft, C. (2011) Progress in understanding of weather systems in West Africa. *Atmospheric Science Letters*, 12, 7–12. <https://doi.org/10.1002/asl.335>.
- Lafore, J.-P., Beucher, F., Peyrillé, P., Diongue-Niang, A., Chapelon, N., Bouniol, D., Caniaux, G., Favot, F., Ferry, F., Guichard, F., Poan, E., Roehrig, R. and Vischel, T. (2017) A multi-scale analysis of the extreme rain event of Ouagadougou in 2009. *Quarterly Journal of the Royal Meteorological Society*, 143, 3094–3109. <https://doi.org/10.1002/qj.3165>.
- Lebel, T., Parker, D.J., Flamant, C., Bourles, B., Marticorena, M., Mougou, E., Peugeot, C., Diedhiou, A., Haywood, J.M., Ngamini, J.B., Polcher, J., Redelsperger, J.L. and Thorncroft, C.D. (2010) The AMMA field campaigns: multiscale and multidisciplinary observations in the West African region. *Quarterly Journal of the Royal Meteorological Society*, 136(S1), 8–33. <https://doi.org/10.1002/qj.486>.
- Lemburg, A., Bader, J. and Claussen, M. (2019) Sahel rainfall–tropical easterly jet relationship on synoptic to intraseasonal time scales. *Journal of Climate*, 147, 1733–1752. <https://doi.org/10.1175/MWR-D-18-0254.1>.
- van der Linden, R., Fink, A.H. and Redl, R. (2015) Satellite-based climatology of low-level continental clouds in southern West Africa during the summer monsoon season. *Journal of Geophysical Research: Atmospheres*, 120, 1186–1201. <https://doi.org/10.1002/2014JD022614>.
- Lohou, F., Kalthoff, N., Adler, B., Babić, K., Dione, C., Lothon, M., Pedruzo-Bagazgoitia, X. and Zouzoua, M. (2020) Conceptual model of diurnal cycle of stratiform low-level clouds over southern West Africa. *Atmospheric Chemistry and Physics*, 20, 2263–2275. <https://doi.org/10.5194/acp-20-2263-2020>.
- Louvet, S., Sultan, B., Janicot, S., Kamsu-Tamo, P.H. and Ndiaye, O. (2016) Evaluation of TIGGE precipitation forecasts over West Africa at intraseasonal timescale. *Climate Dynamics*, 47, 31–47. <https://doi.org/10.1007/s00382-015-2820-x>.
- Maranan, M. and Fink, A.H. (2016) *Radiosonde – all sites*. SEDOO OMP. <https://doi.org/10.6096/baobab-dacciwa.1656>.
- Maranan, M., Fink, A.H. and Knippertz, P. (2018) Rainfall types over southern West Africa: objective identification, climatology and synoptic environment. *Quarterly Journal of the Royal Meteorological Society*, 144(714), 1628–1648.
- Maranan, M., Fink, A.H., Knippertz, P., Francis, S.D., Akpo, A.B., Jegede, G. and Yorke, C. (2019) Interactions between convection and a moist vortex associated with an extreme rainfall event over southern West Africa. *Monthly Weather Review*, 147, 2309–2328. <https://doi.org/10.1175/MWR-D-18-0396.1>.
- Marsham, J.H., Dixon, N.S., Garcia-Carreras, L., Lister, G.M.S., Parker, D.J., Knippertz, P. and Birch, C.E. (2013) The role of moist convection in the West African monsoon system – insights from continental-scale convection-permitting simulations. *Geophysical Research Letters*, 40, 1843–1849. <https://doi.org/10.1002/grl.50347>.
- Mathon, V., Laurent, H. and Lebel, T. (2002) Mesoscale convective system rainfall in the Sahel. *Journal of Applied Meteorology and Climatology*, 41, 1081–1092. [https://doi.org/10.1175/1520-0450\(2002\)041<1081:MCSRIT>2.0.CO;2](https://doi.org/10.1175/1520-0450(2002)041<1081:MCSRIT>2.0.CO;2).
- Milton, S., Diongue-Niang, A., Lamptey, B., Bain, C., Birch, C. and Bougeault, P. (2017) Numerical weather prediction over Africa. In: Parker, D.J. and Diop-Kane, M. (Eds.), chapter 10 *Meteorology of Tropical West Africa: The Forecasters' Handbook*. Chichester, UK: Wiley, pp. 380–422.
- Mohr, K.I. and Thorncroft, C.D. (2006) Intense convective systems in West Africa and their relationship to the African easterly

- jet. *Quarterly Journal of the Royal Meteorological Society*, 132, 163–176. <https://doi.org/10.1256/qj.05.55>.
- Pante, G. and Knippertz, P. (2019) Resolving Sahelian thunderstorms improves mid-latitude weather forecasts. *Nature Communications*, 10, 3487. <https://doi.org/10.1038/s41467-019-11081-4>.
- Parker, D.J. and Diop-Kane, M. (Eds.). (2017) *Meteorology of Tropical West Africa: The Forecasters' Handbook*. Chichester, UK: Wiley.
- Parker, D.J., Fink, A.H., Janicot, S., Ngamini, J.B., Douglas, M., Afiesimama, E., Agustí-Panareda, A., Beljaars, A., Dide, F., Diedhiou, A., Lebel, T., Polcher, J., Redelsperger, J.L., Thorncroft, C. and Wilson, G.A. (2008) The AMMA radiosonde program and its implications for the future of atmospheric monitoring over Africa. *Bulletin of the American Meteorological Society*, 89, 1015–1027. <https://doi.org/10.1175/2008BAMS2436.1>.
- Roberts, A.J., Marsham, J.H. and Knippertz, P. (2015) Disagreements in low-level moisture between (re)analyses over summertime West Africa. *Monthly Weather Review*, 143, 1193–1211. <https://doi.org/10.1175/MWR-D-14-00218.1>.
- Satgé, F., Defrance, D., Sultan, B., Bonnet, M.-P., Seyler, F., Rouché, N., Pierron, F. and Paturel, J.-E. (2020) Evaluation of 23 gridded precipitation datasets across West Africa. *Journal of Hydrology*, 581, 124412. <https://doi.org/10.1016/j.jhydrol.2019.124412>.
- Schrage, J.M. and Fink, A.H. (2012) Nocturnal continental low-level stratus over tropical West Africa: observations and possible mechanisms controlling its onset. *Monthly Weather Review*, 140, 1794–1809. <https://doi.org/10.1175/MWR-D-11-00172.1>.
- Schuster, R., Fink, A.H. and Knippertz, P. (2013) Formation and maintenance of nocturnal low-level stratus over the southern West African monsoon region during AMMA 2006. *Journal of the Atmospheric Sciences*, 70, 2337–2355. <https://doi.org/10.1175/JAS-D-12-0241.1>.
- Selz, T. and Craig, G.C. (2005) Upscale error growth in a high-resolution simulation of a summertime weather event over Europe. *Monthly Weather Review*, 143, 813–827. <https://doi.org/10.1175/MWR-D-14-00140.1>.
- Söhne, N., Chaboureaud, J.-P. and Guichard, F. (2008) Verification of cloud cover forecast with satellite observation over West Africa. *Monthly Weather Review*, 136, 4421–4434. <https://doi.org/10.1175/2008MWR2432.1>.
- Stoffelen, A., Pailleux, J., Källén, E., Vaughan, J.M., Isaksen, L., Flamant, P., Wergen, W., Andersson, E., Schyberg, H., Culoma, A., Meynard, R., Endemann, M. and Ingmann, P. (2005) The atmospheric dynamics mission for global wind field measurement. *Bulletin of the American Meteorological Society*, 86, 73–88. <https://doi.org/10.1175/BAMS-86-1-73>.
- Thiemig, V., Rojas, R., Zambrano-Bigiarini, M., Levizzani, V. and de Roo, A. (2012) Validation of satellite-based precipitation products over sparsely gauged African river basins. *Journal of Hydrometeorology*, 13, 1760–1783. <https://doi.org/10.1175/JHM-D-12-032.1>.
- Tompkins, A.M., Diongue-Niang, A., Parker, D.J. and Thorncroft, C.D. (2005) The African easterly jet in the ECMWF Integrated Forecast System: 4D-Var analysis. *Quarterly Journal of the Royal Meteorological Society*, 131, 2861–2885. <https://doi.org/10.1256/qj.04.136>.
- Vogel, P., Knippertz, P., Fink, A.H., Schlueter, A. and Gneiting, T. (2018) Skill of global raw and postprocessed ensemble predictions of rainfall over northern tropical Africa. *Weather and Forecasting*, 33, 369–388. <https://doi.org/10.1175/WAF-D-17-0127.1>.
- Žagar, N., Gustafsson, N. and Källén, E. (2004) Variational data assimilation in the tropics: the impact of a background-error constraint. *Quarterly Journal of the Royal Meteorological Society*, 130, 103–125. <https://doi.org/10.1256/qj.03.13>.
- Žagar, N., Stoffelen, A., Marseille, G., Accadia, C. and Schlüssel, P. (2008) Impact assessment of simulated Doppler wind lidars with a multivariate variational assimilation in the Tropics. *Monthly Weather Review*, 136, 2443–2460. <https://doi.org/10.1175/2007MWR2335.1>.
- Žagar, N., Buizza, R. and Tribbia, J. (2015) A three-dimensional multivariate modal analysis of atmospheric predictability with application to the ECMWF ensemble. *Journal of the Atmospheric Sciences*, 72, 4423–4444. <https://doi.org/10.1175/JAS-D-15-0061.1>.
- Žagar, N., Horvat, M., Zaplotnik, Ž. and Magnusson, L. (2017) Scale-dependent estimates of the growth of forecast uncertainties in a global prediction system. *Tellus A*, 69(1), 1287492. <https://doi.org/10.1080/16000870.2017.1287492>.
- Zhang, F., Bei, N., Rotunno, R., Snyder, C. and Epifanio, C.C. (2007) Mesoscale predictability of moist baroclinic waves: convection-permitting experiments and multistage error growth dynamics. *Journal of the Atmospheric Sciences*, 64, 3579–3594. <https://doi.org/10.1175/JAS4028.1>.

How to cite this article: van der Linden R, Knippertz P, Fink AH, Ingleby B, Maranan M, Benedetti A. The influence of DACCIWA radiosonde data on the quality of ECMWF analyses and forecasts over southern West Africa. *QJR Meteorol Soc.* 2020;146:1719–1739. <https://doi.org/10.1002/qj.3763>